Inhibition of Human Leukocyte Elastase by N-Substituted Peptides Containing α,α-Difluorostatone Residues at P_1

Jerry W. Skiles,*,†,‖ Clara Miao,† Ronald Sorcek,† Stephen Jacober,† Philip W. Mui,†,⊥ Grace Chow,‡ Steve M. Weldon,§ Genus Possanza,§ Mark Skoog,‡,# James Keirns,‡ Gordon Letts,§ and Alan S. Rosenthal†

Departments of Medicinal Chemistry, Biochemistry, and Pharmacology, Boehringer Ingelheim Pharmaceuticals, Inc., 90 East Ridge, P.O. Box 368, Ridgefield, Connecticut 06877

Received May 6, 1992

A series of tripeptides which contain α,α-difluorostatone residues at P_1-P_1' and span the S_3-S_1' subsites have been shown to be potent inhibitors of human leukocyte elastase (HLE). The tripeptides described contain the nonproteinogenic achiral residue *N*-(2,3-dihydro-1*H*-inden-2-yl)glycine at the P_2-position. This residue has previously been shown in the case of HLE to be a good bioisosteric replacement for L-proline. Of the peptides prepared, those which contain the α,α-difluoromethylene keton derivative of L-valine (difluorostatone) are the preferred residue at the P_1-primary specificity position. Substitution at P_1 by the corresponding α,α-difluoromethylene ketones of L-leucine and L-phenylalanine gives inactive compounds. Of the tripeptides described the most potent in vitro compound is ethyl *N*-[*N*-CBZ-L-valyl-*N*-(2,3-dihydro-1*H*-inden-2-yl)glycyl]-4(*S*)-amino-2,2-difluoro-3-oxo-5-methylhexanoate (**17b**) (IC_{50} = 0.635 μM). It is presumed that the inhibitor **17b** interacts with the S_3-S_1' binding regions of HLE. Additionally extended binding inhibitors were prepared which interact with the S_3-S_3' binding subsites of HLE. In order to effect interaction with the S_1'-S_3' subsites of HLE, the leaving group side of cleaved peptides, spacers based upon Gly-Gly, and those linked via the N^ϵ of L-lysine were utilized. One of the most potent extended compounds (P_3-P_3') in vitro is methyl N^6-[4(*S*)-[[*N*-[*N*-CBZ-L-valyl-*N*-(2,3-dihydro-1*H*-inden-2-yl)glycyl]amino]-2,2-difluoro-3-oxo-5-methylhexanoyl]-2(*S*)-(acetylamino)-6-aminohexanoate (**24b**) (IC_{50} = 0.057 μM). The described in vitro active inhibitors were also evaluated in hamsters in an elastase-induced pulmonary hemorrhage (EPH) model. In this model, intratracheal (it.) administration of **22c**, 5 min prior to HLE challenge (10 μg, it.) effectively inhibited hemorrhage (94.6%) in a dose-dependent manner. The described α,α-difluoromethylene ketone inhibitors are assumed to act as transition-state analogs. The inhibition process presumably acts via hemiketal formation with the active site Ser^{195} of HLE, and is facilitated by the strongly electron withdrawing effect of the α,α-difluoromethylene functionality.

Elastases are a family of proteinases that hydrolytically degrade elastin, a structural protein that is a flexible, highly cross-linked protein which is insoluble in neutral aqueous media and is generally resistant to proteolysis. Imbalances in the levels or regulation of tissue or cellular proteases are thought to manifest themselves in various disease states. Human leukocyte elastase (HLE; EC 3.4.21.37) is a glycosylated, strongly basic serine protease with a molecular weight of approximately 30 kDa, and is found in the azurophilic granules of polymorphonuclear leukocytes (PMN). The complete amino acid sequence of HLE has been determined.[1] This enzyme is released from PMN upon inflammatory stimuli and has been implicated as a pathogenic agent in a number of disease states such as pulmonary emphysema,[2] rheumatoid arthritis,[3] adult respiratory distress syndrome (ARDS),[4] glomerulonephritis,[5] periodontitis, arteriosclerosis, septicemia and shock, and cystic fibrosis.[6]

In order to prevent self-inflicted tissue damage due to enzymes being accidentally released, numerous endogenous inhibitors directed against neutrophil proteinases exist. In the case of HLE, the major endogenous inhibitor is α_1-proteinase inhibitor (α_1-PI). Extracellular HLE is normally inhibited by α_1-PI; however, this delicate balance between proteinase and inhibitor may be disturbed by a genetic defect leading to a decrease in α_1-PI or to the oxidative destruction of α_1-PI. Cigarette smoke, which has been shown to inactivate α_1-PI in vitro (through oxidation of Met^{358}),[7] is believed to cause a localized, functional deficiency of the protease inhibitor. This, in

* Author to whom correspondence should be addressed.
† Department of Medicinal Chemistry.
‡ Department of Biochemistry.
§ Department of Pharmacology.
‖ Present address: CIBA-GEIGY Corp., Pharmaceuticals Division, 556 Morris Ave., Summit, NJ 07901.
⊥ Present address: Schering-Plough Research, Biotechnology Department, 60 Orange St., Bloomfield, NJ 07003.
Present address: Bristol-Myers Squibb Pharmaceutical Research Institute, P.O. Box 4000, Princeton, NJ 08543.

(1) Sinha, S.; Watorek, W.; Karr, S.; Giles, J.; Bode, W.; Travis, S. Primary Structure of Human Neutrophil Elastase. *Proc. Natl. Acad. Sci. U.S.A.* **1987**, *84*, 2228–2232.
(2) Janoff, A. Elastase and Emphysema. Current Assessment of the Protective-Antiprotease Hypothesis. *Am. Rev. Respir. Dis.* **1985**, *132*, 417–433.
(3) Ekerot, L.; Ohlsson, K. Interactions of Granulocyte Proteases with Inhibitors in Rheumatoid-Arthritis. *Adv. Exp. Med. Biol.* **1984**, *167*, 335–344.
(4) Merritt, T. A.; Cochrane, C. G.; Holcomb, K.; Bohl, B.; Hallman, M.; Strayer, D.; Edwards, D.; Gluck, L. Elastase and α_1-PI Proteinase Inhibitor Activity in Tracheal Aspirates During Respiratory Distress Syndrome. *J. Clin. Invest.* **1983**, *72*, 656–666.
(5) Sanders, E.; Davies, M.; Coles, A. On the Pathogenesis of Glomerulonephritis: A Clinico-Pathological Study Indicating that Neutrophils Attack and Degrade Glomerular Basement Membrane. *Renal Physiol.* **1980**, *3*, 335–359.
(6) (a) Jackson, A. H.; Hill, S. L.; Afford, S. C.; Stockley, R. A. Sputum Soluble Phase Proteins and Elastase Activity in Patients with Cystic Fibrosis. *J. Respir. Dis.* **1984**, *65*, 114–124. (b) Suter, S.; Schaad, L.; Roux, L.; Nydegger, V. E.; Waldvogel, F. A. Granulocyte Neutral Proteases and Pseudomonas Elastase as Possible Causes of Airway Damage in Patients with Cystic Fibrosis. *J. Infect. Dis.* **1984**, *149*, 523–531.
(7) Johnson, D.; Travis, J. Structural Evidence for Methionine at the Reactive Site of Human α-1-Proteinase Inhibitor. *J. Biol. Chem.* **1978**, *253*, 7142–7144.

0022-2623/92/1835-4795$03.00/0

turn, is thought to be a primary factor in the pathogenesis of centrilobular emphysema associated with cigarette smoking. Low molecular weight protease inhibitors as therapeutic agents may thus be beneficial as a replacement or supplement to α_1-PI. Of the numerous classes of inhibitors reported, the two most exciting classes are cephalosporins[8] and peptidyl trifluoromethyl ketones[9-12] as is exemplified by 1 and 2 respectively.

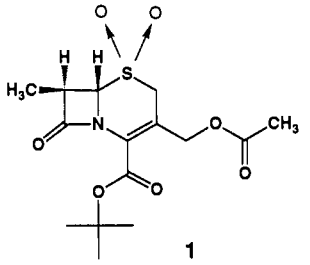

1

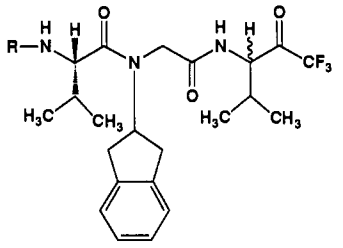

2; R = CBZ

3; R = p-[p-Cl(C_6H_4)SO_2NHCO](C_6H_4)CO

We,[9-11] as well as others,[12] have recently shown that peptidyl trifluoromethyl ketones (e.g., 2 and 3) are potent and specific in vitro inhibitors of HLE. Furthermore, in an in vivo model of elastase-induced emphysema, 3 administered intratracheally (it.) after elastase challenge has been demonstrated to halt the progression of HLE-induced emphysemalike lesions (ED_{50} = 3.8 μg/hamster).[13]

Peptidyl trifluoromethyl ketone inhibitors such as 2 and 3 are presumed to act as structural analogs of the tetrahedral intermediate formed during hydrolysis of a peptide bond. Peptidyl trifluoromethyl ketones such as 2 and 3 may deactivate HLE via transition-state inhibition by two potential means. Both di- and trifluoromethyl ketones exist in water almost entirely in the hydrated form, i.e. as the hemiketal. This tetrahedral hemiketal formation is facilitated by an enzyme-catalyzed reaction (e.g., upon binding to HLE). This hydration of an amino acid ketone is facilitated by placement of electron-withdrawing fluorine atoms adjacent to the carbonyl to give either di- or trifluoromethyl ketones. Alternatively the enhanced electrophilicity of fluorinated ketones over unfluorinated ketones may also facilitate an enzyme-catalyzed addition of the active site Ser^{195} to the ketone carbonyl to form a metastable hemiketal, which resembles the tetrahedral intermediate in the reaction pathway for enzyme-substrate hydrolysis. Although di- and trifluoromethyl ketone inhibitors are assumed to form a covalent bond via hemiketal formation with active site Ser^{195} of HLE, this process is reversible. In the case of porcine pancreatic elastase (PPE), it has been unequivocally demonstrated[14] through X-ray analysis that, in the adducts formed between the enzyme and peptidyl trifluoromethyl ketone inhibitors, the O^{γ} atom of the catalytic Ser^{195} residue is covalently attached (1.5 Å) to the ketone carbonyl of the inhibitor via a hemiketal.

Most of the peptide-based inhibitors described to date occupy maximally the S_1-S_4 binding subsites[15] of the proteolytic enzyme and do not profit from the numerous possible interactions with binding subsites on the "leaving-group" side of the cleaved peptides (i.e., the P_1'-P_3' subsites). Small synthetic inhibitors of HLE that interact in this extended manner have not been reported. In the present work we describe our work in successfully extending the trifluoromethyl ketone inhibitors 2 and 3 into the S'-region of HLE by replacing one of the fluorines of 2 and 3 by an ethoxycarbonyl functionality (e.g., COOEt) and in using this functionality as a handle to further extend into the S_3'-subsite region. This functionality has been successfully used by us to gain further enzyme–ligand interactions by the interaction with remote residues. Crystallographic studies on serine proteases bound to natural protein inhibitors indicate that the limit of the binding cleft is at the S_3'-subsite. In order to potentially facilitate a P_3'-S_3' inhibitor–enzyme interaction, molecular modeling in conjunction with X-ray crystallography was utilized to evaluate appropriate spacing groups. Furthermore, prior work has also provided evidence that S'-interactions are important in naturally occurring inhibitors of serine protease such as turkey ovomucoid (OMTKY3).[16] The bulk of chemical structural literature on HLE refers to inhibitors or ligands lacking S'-functionality; thus, much

(8) Doherty, J. B.; Ashe, B. M.; Argenbright, L. W.; Barker, P. L.; Bonney, R. J.; Chandler, G. O.; Dahlgren, M. E.; Dorn, C. P., Jr.; Finke, P. E.; Firestone, R. A.; Fletcher, D.; Hagmann, W. K.; Mumford, R.; O'Grady, L.; Maycock, A. L.; Pisano, J. M.; Shah, S. K.; Thompson, K. R.; Zimmerman, M. Cephalosporin Antibiotics Can be Modified To Inhibit Human Leukocyte Elastase. *Nature* **1986**, *322*, 192–194.

(9) Skiles, J. W.; Fuchs, V.; Chow, G.; Skoog, M. Inhibition of Human Leukocyte Elastase by N-Substituted Tripeptide Trifluoromethyl Ketones. *Res. Commun. Chem. Pathol. Pharmacol.* **1990**, *68*, 365–374.

(10) Skiles, J. W.; Fuchs, V.; Miao, C.; Sorcek, R.; Grozinger, K. G.; Mauldin, S. C.; Vitous, J.; Mui, P. W.; Jacober, S.; Chow, G.; Matteo, M.; Skoog, M.; Weldon, S. M.; Possanza, G.; Keirns, J.; Letts, G.; Rosenthal, A. S. Inhibition of Human Leukocyte Elastase (HLE) by N-Substituted Peptidyl Trifluoromethyl Ketones. *J. Med. Chem.* **1992**, *35*, 641–662.

(11) Skiles, J. W.; Fuchs, V.; Leonard, S. F. Imidazo[1,2-a]Piperazines as Mechanistic Inhibitors of Serine Proteinases. *Bioorg. Med. Chem. Lett.* **1991**, *1*, 69–72.

(12) (a) Gelb, M. H.; Svaren, J. P.; Abeles, R. H. Fluoro Ketone Inhibitors of Hydrolytic Enzymes. *Biochemistry* **1985**, *24*, 1813–1817. (b) Imperiali, B.; Abeles, R. H. Inhibition of Serine Proteases by Peptidyl Fluoromethyl Ketones. *Biochemistry* **1986**, *25*, 3760–3767. (c) Imperiali, B.; Abeles, R. H. A. Versatile Synthesis of Peptidyl Fluoromethyl Ketones. *Tetrahedron Lett.* **1986**, *27*, 135–138. (d) Dunlap, R. P.; Stone, P. J.; Abeles, R. H. Reversible Slow, Tight-Binding Inhibition of Human Leukocyte Elastase. *Biophys. Res. Commun.* **1987**, *145*, 509–513. (e) Stein, R. L.; Strimpler, A. M.; Edwards, P. D.; Lewis, J. J.; Mauger, R. C.; Schwartz, J. A.; Stein, M. M.; Trainor, D. A.; Wildonger, R. A.; Zottola, M. A. Mechanism of Slow-Binding Inhibition of Human Leukocyte Elastase by Trifluoromethyl Ketones. *Biochemistry* **1987**, *26*, 2682–2689. (f) Peet, N. P.; Burkhart, J. P.; Angelastro, M. R.; Giroux, E. L.; Mehdi, S.; Bey, P.; Kolb, M.; Neises, B.; Schirlin, D. Synthesis of Peptidyl Fluoromethyl Ketones and Peptidyl α-Keto Esters as Inhibitors of Porcine Pancreatic Elastase, Human Neutrophil Elastase, and Rat and Human Neutrophil Cathepsin G. *J. Med. Chem.* **1990**, *33*, 394–407.

(13) Weldon, S. M.; Letts, L. G.; Keirns, J.; Chow, G.; Skoog, M.; Skiles, J.; Fuchs, V.; Possanza, G. J. BIRA-0260XX, [3(RS)-[[4-(4-Chlorophenyl)-sulfonylaminocarbonyl]phenyl-1-Oxomethyl]-L-Valyl-N-(2,3-Dihydro-1H-Inden-2-yl)glycyl-N-[3-(1,1,1-Trifluoro-4-Methyl-2-Oxopentyl)]amide: A Specific, Long Lasting Inhibitor of Human Neutrophil Elastase. *FASEB J.* **1990**, *4*(4), Abstr. 5212.

(14) Takahashi, L. H.; Rosenfield, R. E., Jr.; Meyer, E. F., Jr.; Trainor, D. A.; Stein, M. X-Ray Diffraction Analysis of the Inhibition of Porcine Pancreatic Elastase by a Peptidyl Trifluoromethylketone. *J. Mol. Biol.* **1988**, *201*, 423–428.

(15) The nomenclature used for describing the individual amino acid residues (P_2, P_1, P_1', P_2' etc.) of a peptide substrate and the corresponding subsites (S_2, S_1, S_1', S_2', etc.) of a protease is that of Schecter and Berger: Schecter, I.; Berger, A. On the Size of the Active Site in Proteases. I. Papain. *Biochem. Biophys. Res. Commun.* **1967**, *27*, 157–162.

Table I. In Vitro HLE Inhibitory Activities of N-Substituted Tripeptide Difluoromethylene Ketones

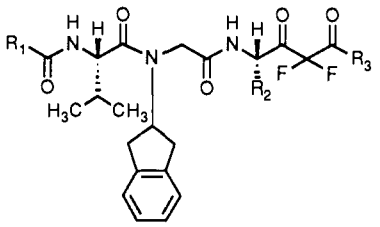

compd[a]	R_1	R_2	R_3	method[b]	formula[c]	IC_{50},[d] μM
22a	*p*-[*p*-Cl(C_6H_4)SO_2NHCO](C_6H_4)	$PhCH_2$	OEt	A–G, M, N	$C_{43}H_{43}ClF_2N_4O_9S$	≫5
17a	$PhCH_2O$	$CH_2CH(CH_3)_2$	OEt	A–H	$C_{34}H_{43}F_2N_3O_7$	11.1
22b	*p*-[*p*-Cl(C_6H_4)SO_2NHCO](C_6H_4)	$CH_2CH(CH_3)_2$	OEt	A–G, M, N	$C_{40}H_{43}ClF_2N_4O_9S$	4.9
17b	$PhCH_2O$	$CH(CH_3)_2$	OEt	AH	$C_{33}H_{41}F_2N_3O_7$	0.635
19	$PhCH_2O$	$CH(CH_3)_2$	OH	A–I	$C_{31}H_{39}F_2N_3O_7$	≫5
22c	*p*-[*p*-Cl(C_6H_4)SO_2NHCO](C_6H_4)	$CH(CH_3)_2$	OEt	A–G, M, N	$C_{39}H_{43}ClF_2N_4O_9S$	0.404
23b	$PhCH_2O$	$CH(CH_3)_2$	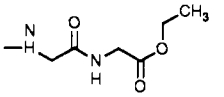	A–E, L	$C_{37}H_{47}F_2N_5O_9$	0.069
24b	$PhCH_2O$	$CH(CH_3)_2$	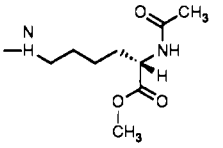	A–E, J, K	$C_{40}H_{53}F_2N_5O_9$	0.057
1[e]						0.107
2[f]						0.365
3[g]						0.084

[a] All compounds are of the (*S*)-configuration at P_3 and P_1. [b] See Experimental Section. [c] All compounds exhibited satisfactory C, H, and N microanalyses and were within 0.4% of theoretical values. All compounds exhibited ^1H NMR and MS spectra consistent with the assigned structures. [d] Concentration inhibiting 50% of the activity of HLE at pH 7.5 in 0.1 M Tris buffer containing 0.5 M NaCl with the substrate MeO-Suc-Ala-Ala-Pro-Val-*p*NA at a concentration of 0.5 mM. Compounds and HLE were incubated for 20 min prior to starting the reaction by addition of substrate. Initial rates were linear in each case. [e] Literature[8] IC_{50} = 1.33 μM. [f] Literature[10] IC_{50} = 0.365 μM. [g] Literature[10] IC_{50} = 0.084 μM.

less is known about receptor–ligand interactions in the P′ "leaving group" side.

Our working hypothesis was that additional interactions between the S′-subsites of the enzyme and the P′-fragments of the peptidyl difluoro ketone inhibitors may contribute to overall tight binding. It was also believed that targeted syntheses in the prime region could provide improved S′-P′ interactions which may in turn provide enhanced specificity and potency.

Chemistry

Compounds of Table I were conveniently prepared as is illustrated in Schemes I–III. The suitably protected statine[17,18] derivatives **7** were prepared as is shown in Scheme I. The *t*-BOC amino acids **4** were coupled with

Scheme I [a]

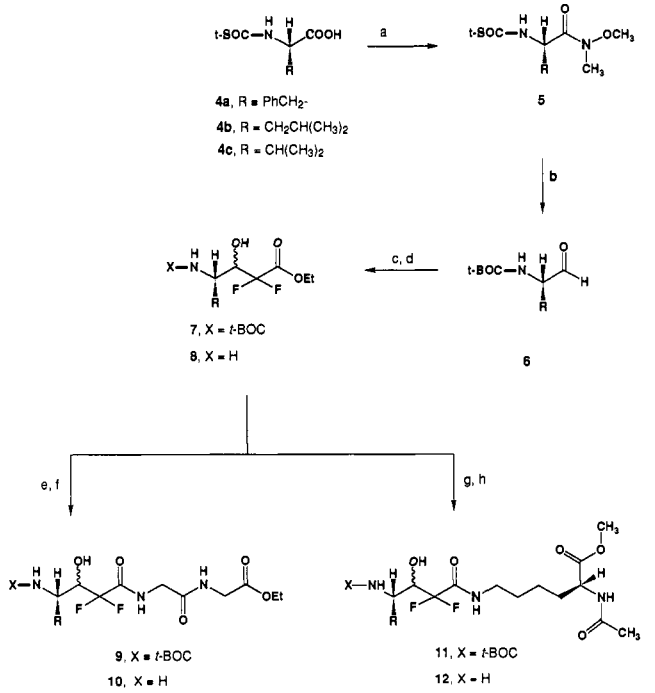

[a] Reagents: (a) CDI, $HN(OCH_3)(CH_3)$, CH_2Cl_2; (b) $LiAlH_4$, THF; (c) Zn, $BrCF_2CO_2Et$, THF to give **7**; (d) **7**, CF_3COOH to give **8**; (e) **7**, $H_2NCH_2CONHCH_2CO_2Et$; (*i*-Pr)$_2$NEt, EtOH to give **9**; (f) **9**, CF_3COOH to give **10**; (g) **7**, N^{α}-acetyl-L-Lys-OCH_3, (*i*-Pr)$_2$NEt, EtOH to give **11**; (h) **11**, CF_3COOH to give **12**.

N,O-dimethylhydroxylamine[19] employing carbonyldiimidazole (CDI) to give the protected amides **5**. The amides **5** were reduced with $LiAlH_4$ to give the protected amino

(16) The X-ray coordinates of HLE complexed with both the chloromethyl ketone inhibitor MeO-Suc-Ala-Ala-Pro-Val chloromethyl ketone and that with the third domain of the natural inhibitor of the turkey ovomucoid inhibitor (OMTKY3) were obtained from the Max Planck Institute (Bode, W., Martinsried, Germany). For discussions on the X-ray analysis as well as a description of the substrate specificity of HLE, see (a) Bode, W.; Meyer, E., Jr.; Powers, J. C. Human Leukocyte and Porcine Pancreatic Elastase: X-ray Crystal Structures, Mechanism, Substrate Specificity, and Mechanism-Based Inhibitors. *Biochemistry* **1989**, *28*, 1951–1963. (b) Bode, W.; Wei, A.-Z.; Huber, R.; Meyer, E.; Travis, J.; Neumann, S. X-Ray Crystal Structure of the Complex of Human Leukocyte Elastase (PMN Elastase) and the Third Domain of the Turkey Ovomucoid Inhibitor. *EMBO* **1986**, *5*, 2453–2458. (c) An-Zhi, W.; Mayr, I.; Bode, W. The Refined 2.3 Å Crystal structure of Human Leukocyte Elastase in a Complex with a Valine Chloromethyl Ketone Inhibitor. *FEBS Lett.* **1988**, *234*, 367–373.

(17) Thaisrivongs, S.; Pals, D. T.; Kati, W. M.; Turner, S. R.; Thomasco, L. M. Difluorostatine- and Difluorostatone-Containing Peptides as Potent and Specific Renin Inhibitors. *J. Med. Chem.* **1985**, *28*, 1553–1555.

(18) Thaisrivongs, S.; Pals, D. T.; Kati, W. M.; Turner, S. R.; Thomasco, L. M.; Watt, W. Design and Synthesis of Potent and Specific Renin Inhibitors Containing Difluorostatine, Difluorostatone, and Related Analogues. *J. Med. Chem.* **1986**, *29*, 2080–2087.

Scheme II [a]

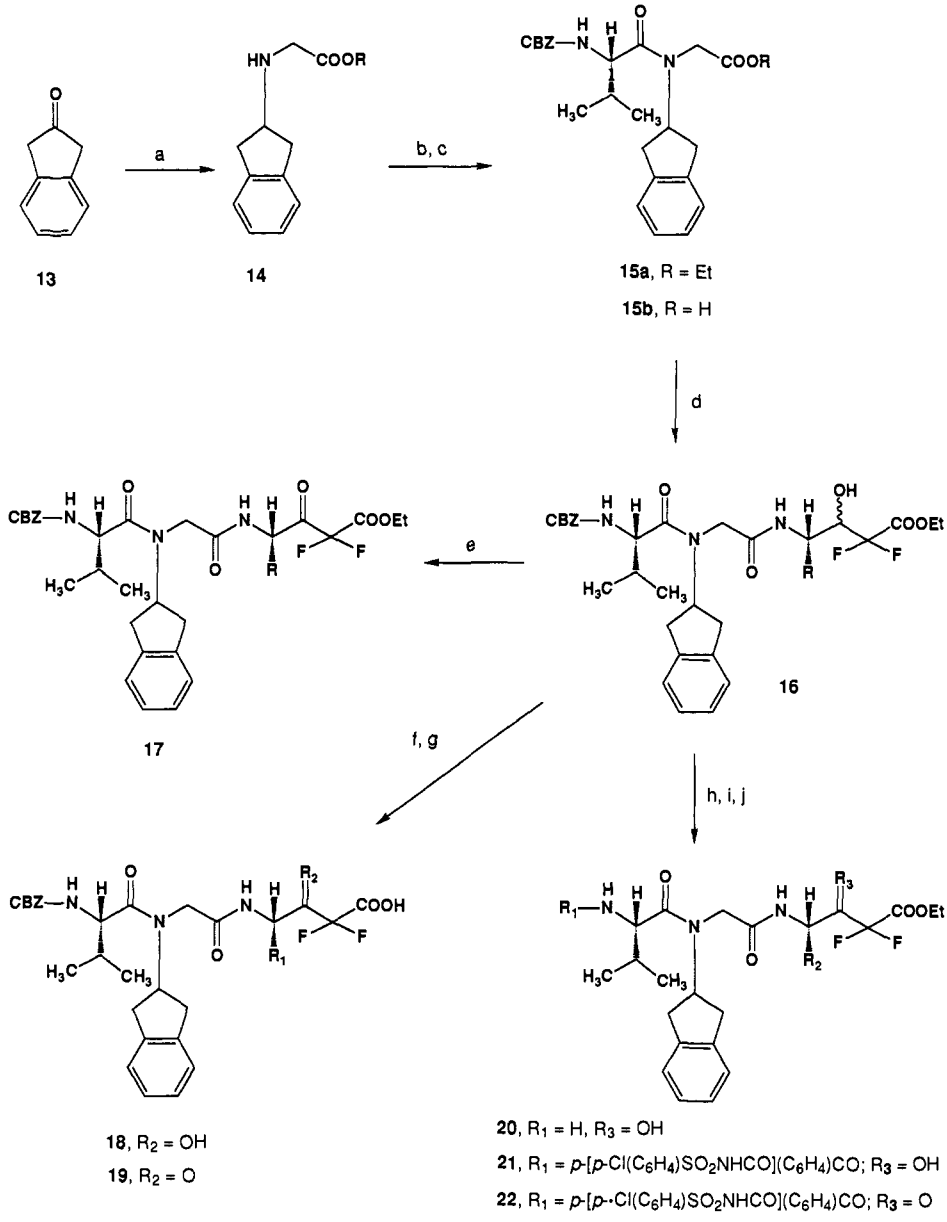

[a] Reagents: (a) $H_2NCH_2CO_2Et$, $NaBH_3CN$, EtOH; (b) CBZ-L-valine, CDI, CH_2Cl_2 to give **15a**; (c) **15a**, KOH, EtOH to give **15b**; (d) **8**, **15b**, WSCDI, HOBT, THF; (e) Dess–Martin periodinane, CF_3COOH, CH_2Cl_2; (f) KOH, EtOH to give **18**; (g) **18**, Dess–Martin periodinane, CF_3COOH, CH_2Cl_2 to give **19**; (h) 10% Pd/C, H_2 (45 psi), EtOH, to give **20**; (i) **20**, p-[p-Cl(C_6H_4)SO_2NHCO](C_6H_4)COOH, WSCDI, HOBT, THF to give **21**; (j) **21**, Dess–Martin periodinane, CF_3COOH, CH_2Cl_2 to give **22**.

acid aldehydes **6**.[20] A Reformatsky reaction of the *t*-BOC aldehydes **6** with ethyl bromodifluoroacetate in the presence of activated zinc dust afforded the diastereomeric alcohols **7**, which were used directly without further purification. Deprotection of the *t*-BOC alcohols **7** with CF_3COOH gave the amino alcohols **8** as their trifluoroacetate salts.

In order to extend the potential inhibitors into the S_1'-S_3' subsites, the statine derivatives **10** (R = $CH(CH_3)_2$) and **12** (R = $CH(CH_3)_2$) were prepared as is illustrated in Scheme I. Treatment of the *t*-BOC-α,α-difluorostatine ethyl ester **7** with ethyl glycylglycinate in refluxing EtOH afforded the protected amides **9**, which ultimately corresponds to a P_1-P_3' spacer link in the inhibitor **23b**. Treatment of **9** with CF_3COOH effected the removal of the *t*-BOC group to give the amine **10**. In a similar manner, treatment of the protected α,α-difluorostatine analog **7** with N^{α}-acetyl-L-lysine ethyl ester in refluxing EtOH gave, after deprotection with CF_3COOH, the amino alcohol **12** as a mixture of diasteriomers which were used directly without further purification. The amide **12** ultimately corresponds to the P_1-P_3' tether in the extended inhibitor **24b**.

The N-substituted tripeptide inhibitors **17** and **22** were prepared by standard peptide coupling and deprotection procedures as is illustrated in Scheme II. In our study nonproteinogenic achiral N-substituted glycine residues were utilized at P_2, in particular *N*-(2,3-dihydro-1*H*-inden-2-yl)glycine (**14**). We have previously shown[9,10] that in the case of trifluoromethyl ketone inhibitors this residue may replace L-proline to give potent and specific inhibitors of HLE that possess long duration of action in an in vivo

(19) Nahm, S.; Weinreb, S. M. *N*-Methoxy-*N*-Methylamides as Effective Acylating Agents. *Tetrahedron Lett.* **1981**, *22*, 3815–3818.

(20) Fehrentz, J. A.; Castro, B. An Effective Synthesis of Optically Active α-(*t*-Butoxycarbonylamino)-aldehydes from α-Amino Acids. *Synthesis* **1983**, 676–678.

model of elastase induced pulmomary hemorrhage. Ethyl *N*-(2,3-dihydro-1*H*-inden-2-yl)glycinate (**14**) was prepared by treatment of a mixture of 2-indanone (**13**) and glycine ethyl ester hydrochloride in EtOH with $NaCNBH_3$. The required dipeptide ester **15a** was prepared via a CDI-mediated condensation between *N*-CBZ-L-valine and **14** in CH_2Cl_2 or THF. The dipeptide ester **15a** was hydrolyzed to the corresponding dipeptide acid **15b** with KOH in EtOH. The acid **15b** was then condensed with the α,α-difluorostatine ethyl ester derivatives **8** via a water-soluble carbonyl diimide (WSCDI) reagent, 1-[3-(dimethylamino)-propy]-3-ethylcarbodiimide, in THF as the amide-forming reagent to give the tripeptides **16** as a mixture of diastereomers which were used directly without separation. The *N*-CBZ-protected tripeptides **16** were oxidized to the corresponding α,α-difluoromethylene ketones **17** by Dess–Martin periodinane.[21] Treatment of the tripeptide esters **16** with 1 equiv of KOH in EtOH gave the alcohol acids **18**, which were then oxidized via Dess–Martin periodinane to the α,α-difluoromethylene keto acid **19**.

In order to extend the tripeptides **16** into the S_5-S_4 subsite region the amino terminal alcohols **20** were required. The *N*-CBZ tripeptides **16** were deprotected catalytically over 10% Pd/C (H_2, 45 psi) in EtOH to give the amines **20**. The tripeptides **20** were condensed with the acid[10,22,23] *p*-[*p*-Cl(C_6H_4)SO_2NHCO](C_6H_4)CO_2H using WSCDI/HOBT to give the alcohols **21**, which were then oxidized by Dess–Martin periodinane[21] to afford the α,α-difluoromethylene ketones **22**.

The extended binding inhibitors **23b** and **24b** were prepared as shown in Scheme III. Condensation of the *N*-CBZ tripeptide acid **15b** with the amine **10** in the presence of WSCDI/HOBT gave **23a** as a mixture of diastereomers which were used directly without further separation. Oxidation of the diastereomeric alcohols **23a** with Dess–Martin periodinane gave the ketone **23b**. In a similar manner the ketone **24b** was efficiently obtained by condensing the acid **15b** with the amine **12** in the presence of WSCDI/HOBT to give, after Dess–Martin periodinane oxidation, **24b**.

Results and Discussion

The compounds presented in Table I represent a novel peptidyl series of potent and specific human leukocyte elastase (HLE) inhibitors which contain derivatives of α,α-fluorostatone at P_1-P_1'. The peptides described contain L-valine at P_3 and the nonproteinogenic achiral residue *N*-(2,3-dihydro-1*H*-inden-2-yl)glycine at the P_2-position. This N-substituted glycine residue has previously been shown[9,10] in the case of trifluoromethyl ketone inhibitors of HLE to be a good bioisosteric replacement for L-proline.

Scheme III [a]

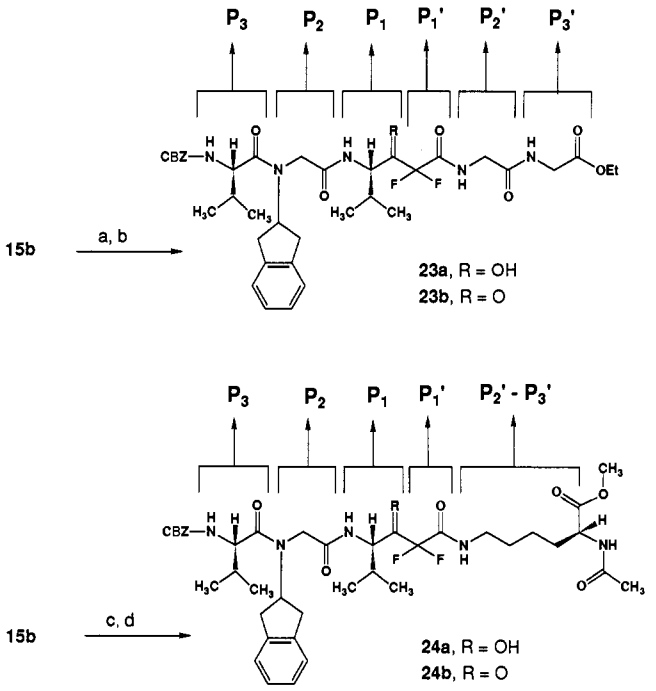

[a] Reagents: (a) **15b**, **10**, WSCDI, HOBT to give **23a**; (b) Dess–Martin periodinane, CF_3COOH, CH_2Cl_2 to give **23b**; (c) **15b**, **12**, WSCDI, HOBT to give **24a**; (d) Dess–Martin periodinane, CF_3COOH, CH_2Cl_2 to give **24b**.

As is seen from the Table I, the α,α-difluoromethylene ketone (difluorostatone) derivative of L-valine, e.g. **17b** and **22c** (IC_{50} = 0.635 and 0.404 μM, respectively), is the preferred residue at the P_1-primary specificity position of the inhibitors described herein. Substitution at P_1-P_1' by the corresponding α,α-difluoromethylene ketones of L-leucine to give **17a** and **22b** (IC_{50} = 11.1 and 4.9 μM, respectively) or by that of L-phenylalanine to give **22a** (IC_{50} = $\gg$5 μM) all afford less active compounds when compared to the P_1-P_1' L-valine derivative **22c** (IC_{50} = 0.404 μM). The inhibitors **17a** and **17b** span the P_3-P_1' subsites whereas the inhibitor **22c** spans the P_5-P_1' subsites and all of these inhibitors contain derivatives of α,α-difluorostatone at P_1-P_1'. The tripeptide **22c** is N-terminated with the functionality *p*-[*p*-Cl(C_6H_4)SO_2NHCO]-(C_6H_4)CO. In accord with our previous report,[9,10] and others,[22] this sulfonamide functionality confers high in vivo activity as well as an enhancement in in vitro potency to peptidyl trifluoromethyl ketones relative to the corresponding CBZ or *t*-BOC derivatives. This is also true in the present report (e.g., α,α-difluoromethylene ketones), as is seen when the homologous series such as **17b** (IC_{50} = 0.635 μM) is compared with **22c** (IC_{50} = 0.404 μM). Presumably, this sulfonamide functionality effectively increases binding to HLE through favorable interactions with residues in the S_5-S_4-subsites. Furthermore, in an in vivo situation, the acidic nature of the sulfonamide may prevent the rapid clearance of the inhibitors from the lungs when compared to CBZ N-terminated tripeptides.

From Table I it is seen that besides requiring a derivative of L-valine at P_1 it is crucial that the tripeptides described contain an ester functionality at the carboxy terminal end of the peptide for good in vitro potency. For example, the ethyl ester **17b** has an IC_{50} of 0.635 μM whereas the corresponding carboxylic acid compound **19** is inactive (IC_{50} = $\gg$5 μM). This may not be surprising since it is well-known that HLE prefers small uncharged residues at

(21) Dess, D. B.; Martin, J. C. Readily Accessible 12-I-5 Oxidant for the Conversion of Primary and Secondary Alcohols to Aldehydes and Ketones. *J. Org. Chem.* **1983**, *48*, 4155–4156. **Caution**: Care should be taken in the handling of this reagent. The **explosive** nature of periodinane and its precursor 2-iodoxybenzoic acid has recently been described: Plumb, J. B.; Harper, D. J. *Chem. Eng. News* **1990**, *July 16*, 3.

(22) (a) Krell, R. D.; Stein, R. L.; Strimpler, A. M.; Trainor, D.; Edwards, P.; Wolanin, D.; Wildonger, R.; Schwartz, J.; Hesp, B.; Giles, R. E.; Williams, J. C. Biochemical Characterization of ICI 200,880: A Novel, Potent and Selective Inhibitor of Human Neutrophil Elastase. *FASEB J.* **1988**, *2* (*4*), Abstract 290. (b) Williams, J. C.; Stein, R. L.; Knee, C.; Egan, J.; Falcone, R.; Trainor, D.; Edwards, P.; Wolanin, D.; Wildonger, R.; Schwartz, J.; Hesp, B.; Giles, R. E.; Krell, R. D. Pharmacologic Characterization of ICI 200,880: A Novel Potent and Selective Inhibitor of Human Neutrophil Elastase. *FASEB J.* **1988**, *2* (*4*), Abstr. 291.

(23) Bergeson, S.; Schwartz, J. A.; Stein, M. M.; Wildonger, R. A.; Edwards, P. D.; Shaw, A.; Trainor, D. A.; Wolanin, D. J. EP Patent Appl. 0 189 305, **1986**.

P_1 and the vicinity. We have recently reported[9,10,11] upon peptidyl trifluoromethyl ketones as potent and specific inhibitors of HLE. The primary specificity pocket of HLE (S_1) is hydrophobic, consisting of the residues Val^{190} and Val^{216} of HLE, which may explain the enzyme's preference for hydrophobic, nonpolar, uncharged residues. The loss of potency by the carboxylic acid **19** may simply be the result of placing a very hydrophilic residue (COOH) near or into the hydrophobic S_1-S_1' region, which, by the presence of a negatively charged species, may result in a decrease of hydrophobic interactions between the inhibitor and the enzyme. On the other hand the neutrally charged ethyl ester **17b** is expected to have a favorable hydrophobic interaction with Val^{190} and Val^{216} of HLE.

One of the most potent trifluoromethyl inhibitors reported[9,10] is **3** (BI-RA-260) (IC_{50} = 0.084 μM). The in vitro potency of the trifluoromethyl ketone inhibitor **3** is 1 order of magnitude greater than the corresponding α,α-difluorostatone derivative **22c** (IC_{50} = 0.404 μM). This difference in potency may be due to the overall difference in the electronegative inductive effect of a trifluoromethyl residue when compared to that of a difluoromethylene residue. Presumably the mechanism of inhibition of HLE by trifluoromethyl ketone compounds, such as **2** and **3**, and of α,α-difluoromethylene ketone compounds, such as **17b** and **22c**, is through transition-state inhibition. The enhanced electrophilicity of the fluorinated ketone carbonyl of compounds such as **2** and **3** or **17b** and **22c** facilitates the enzyme-catalyzed addition of active site Ser^{195} to the ketone carbonyl to form a metastable hemiketal, which resembles the tetrahedral intermediate in the reaction pathway for enzyme–substrate hydrolysis. Although the α,α-difluoromethyl ketone inhibitors are assumed to form a covalent bond with the active site Ser^{195} of HLE, this process is reversible. In the case of porcine pancreatic elastase (PPE), it has been unequivocally demonstrated[14] through X-ray analysis that, in the adducts formed between the enzyme and the peptidyl trifluoromethyl ketone inhibitors, the O^{γ} atom of the catalytic Ser^{195} residue covalently attached (1.5 Å) to the ketone carbonyl of the inhibitor via hemiketal formation. A similar type mechanistic inhibition is presumed to be the case with the α,α-difluoromethylene ketone inhibitors described herein. Because of the high electrophilicity of the fluorine atoms, an alternative mechanism may be due to the generation of transition-state inhibitors in situ resulting from the addition of H_2O to the α,α-difluoromethylene ketone.

The X-ray structure of HLE complexed with both synthetic and natural inhibitors has recently become available.[16] In order to gain some molecular insight into the binding properties of extended inhibitors (P_1'-P_3'), and to provide a better understanding of the structure–activity relationships, molecular modeling studies were performed utilizing the X-ray coordinates of the complex of the third domain of the natural inhibitor of the turkey ovomucoid (OMTKY3) with HLE. We have previously shown[10] that if it is assumed on the basis of mechanistic grounds that the carbonyl of the trifluoromethyl ketone of the active inhibitors reacts covalently but reversibly with the active site Ser^{195} of HLE, then it is seen from molecular docking studies that, in order to best fit and have desirable hydrogen-bonding interactions, the bulky substituents on the P_2-glycines of the enzyme–inhibitor complexes must stick out into solution away from the core

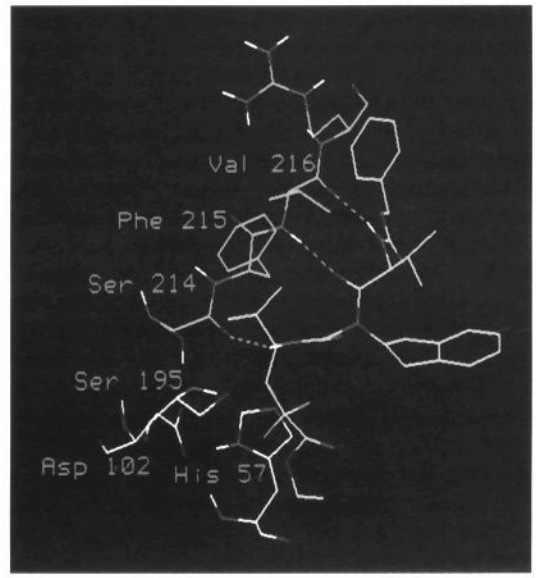

Figure 1. Minimized structure of HLE complexed with the α,α-difluoromethylene inhibitor **17b** detailing the binding and catalytic sites of HLE. The binding residues (Ser^{214}, Phe^{215}, Val^{216}, and Arg^{217}) and the catalytic triad (Ser^{195}, His^{57}, and Asp^{102}) of HLE are given in blue and white, respectively. The inhibitor is shown in yellow. For minimization calculations the constraint (1.78 Å) of covalently linking Ser^{195} with the α,α-difluoromethylene carbonyl of the inhibitor **17b** via hemiketal formation was utilized. Hydrogen bonds formed between HLE residues and those of the inhibitor **17b** are indicated by dotted lines (Val^{216} CO to NH of P_3-Val, 1.83 Å; Val^{216} NH to CO of P_3-Val, 1.90 Å; Ser^{214} CO to NH of P_1-Val, 1.82 Å).

of HLE. Molecular modeling indicates that a similar situation exists in the case of α,α-difluoromethylene ketone inhibitors. Figure 1 shows the catalytic triad (Ser^{195}, Asp^{102}, and His^{57}) of HLE in white and the binding site residues (Val^{216}, Phe^{215}, and Ser^{214}) of HLE in blue. The α,α-difluoromethylene inhibitor **17b** is in yellow. In the binding conformations depicted in Figure 1, the P_1-difluoromethylene ketone carbonyl of the inhibitor **17b** is covalently linked (1.78 Å) to the Ser^{195} of HLE via hemiketal formation. Hydrogen bonds between the HLE binding site residues and those of the inhibitor **17b** are as follows: Val^{216} CO to NH of P_3-Val, 1.83 Å; Val^{216} NH to CO of P_3-Val, 1.90 Å; Ser^{214} CO to NH of P_1-Val, 1.82 Å. The angles of the generated hydrogen bonds between the inhibitor **17b** and HLE are as follows: Val^{216} CO to N of P_3-Val, 164.57°; Val^{216} O to NH of P_3-Val, 169.15°; Val^{216} NH to O of P_3-Val, 166.85°; Val^{216} H to OC of P_3-Val, 167.43°; Ser^{214} CO to N of P_1-Val, 154.80°; Ser^{214} O to HN of P_1-Val, 149.40°. The ethoxy carbonyl of **17b** makes no contribution to the overall binding other than to fit into the hydrophobic S_1'-pocket and thus helps to stabilize the complex.

In order to gain some insight into the possibility of extending the inhibitor **17b** further into the prime region and thus take further advantage of P′-S′-interactions, molecular modeling studies were conducted with the natural inhibitor OMTKY3 and the trifluoromethyl ketone inhibitor **2**. Figure 2 depicts, on the basis of the X-ray structure, how the third domain of the turkey ovomucoid inhibitor aligns itself with the catalytic site of HLE. The catalytic site of HLE (Ser^{195}, Asp^{102}, and His^{57}) is shown in white and the partial structure of OMTKY3 in yellow (residues Pro^{14}-Ala^{15}-Cys^{16}-Thr^{17}-Leu^{18}-Glu^{19}-Tyr^{20}). In this figure the P_1'-Glu^{19i} is within the oxyanion hole of

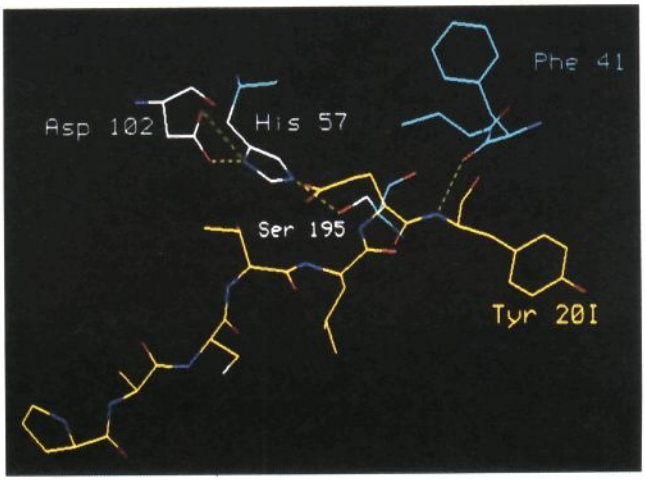

Figure 2. X-ray structure corresponding to a complex between HLE and the third domain of the turkey ovomucoid inhibitor (OMTKY3). The OMTKY residues Pro^{14}-Ala^{15}-Cys^{16}-Thr^{17}-Leu^{18}-Glu^{19}-Tyr^{20} are shown in yellow. The catalytic site of HLE (Asp^{102}, His^{57}, and Ser^{195}) is shown in white and the Phe^{41} binding residue in blue. Donor–acceptor distances between HLE residues and those of OMTKY3 are indicated by dotted lines (P_3'-N to O of Phe^{41}, 3.03 Å). Donor–acceptor distances between residues of the catalytic site are also indicated by dotted lines (O of Asp^{102} to imidazole N of His^{57}, 3.26 Å; O of Asp^{102} to imidazole N of His^{57}, 2.56 Å; N imidazole of His^{57} to O$^{\gamma}$ of Ser^{195}, 2.48 Å).

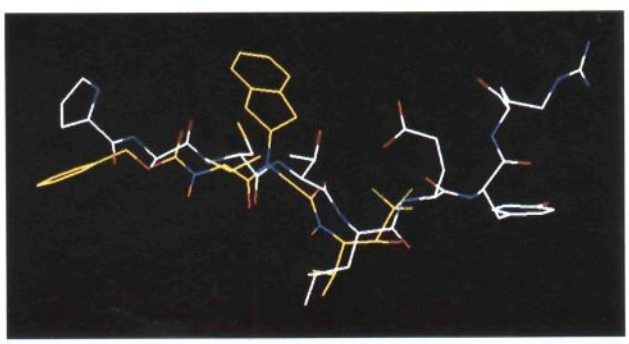

Figure 3. Overlay of **2** in yellow with P_5-P_1' residues of turkey ovomucoid (OMTKY3) in white. The residues Pro^{14}-Ala^{15}-Cys^{16}-Thr^{17}-Leu^{18}-Glu^{19}-Tyr^{20} of OMTKY3 are illustrated.

HLE created by the residues Val^{190}, Val^{216}, and Asp^{226}. From the X-ray structure it is clearly seen that Tyr^{20i} of OMTKY3 makes a very effective hydrogen bond with the carbonyl of Phe^{41} (Phe^{41} CO to NH of P_2'-Tyr^{20i}). The donor–acceptor distance is 3.03 Å (P_3'-N to oxygen of Phe^{41}) and the angle between Phe^{41} CO and the nitrogen of P_2'-Tyr^{20i} is 142.73°. It was thought that the hydrogen bonding that is observed in the natural inhibitor between Phe^{41} and Tyr^{20i} and which is incapable of forming in the trifluoromethyl ketone series of inhibitors (e.g., **2**) might be taken advantage of in the case of the α,α-difluoromethylene series through chain extension. The first step in the design process of preparing inhibitors extended into the S_2'-S_3' region is to utilize molecular modeling to overlay the least energy conformation of the trifluoromethyl ketone **2** with that of OMTKY3 in order to obtain a proper alignment with statone-containing inhibitors which contain one atom less than a true dipeptide mimic. This overlay and alignment is seen in Figure 3. In this figure the following alignment is made: P_3-Val, P_2-(*N*-indanyl)-Gly, and P_3-Val of **2** with P_3-Cys^{16}, P_2-Thr^{17}, and P_1-Leu^{17} of OMTKY3, respectively. The distance from the carbon of the P_1-carbonyl of OMTKY3 (i.e., Leu^{18}) to the oxygen

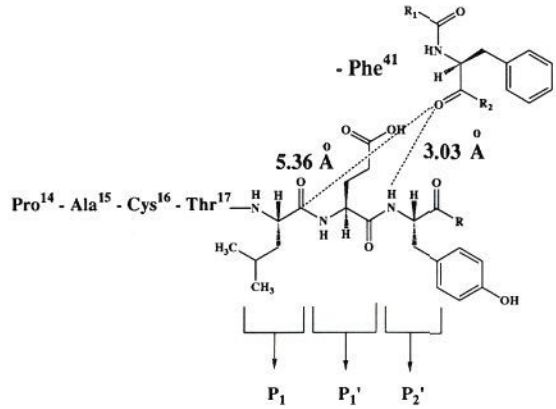

P_2' - N (Tyr^{20i}) to oxygen of Phe^{41} is 3.03 Å.

Figure 4. Schematic representation of the hydrogen-bonding interactions, as taken from the X-ray structure, of turkey ovomucoid (OMTKY3) with Phe^{41} of HLE [P_2'-N (Tyr^{20i}) to the O of Phe^{41} is 3.03 Å)]. The distance from the C of the P_1-CO to the O of Phe^{41} is 5.36 Å.

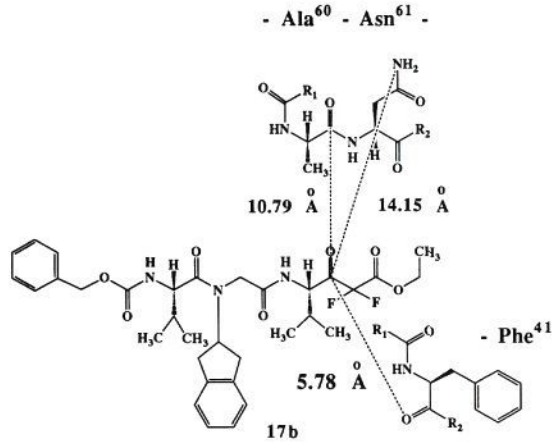

Figure 5. A schematic representation of potential hydrogen-bonding interactions of the inhibitor **17b** with remote residues, i.e. Asn^{61}, Ala^{60}, and Phe^{41}. The following distances are observed: from the carbon of the P_1-CO to the O of Ala^{60}, 10.79 Å; from the C of the P_1-CO to the side-chain N of Asn^{60}, 14.15 Å; from the carbon of the P_1-CO to the O of Phe^{41}, 5.78 Å.

of Phe^{41} of HLE is 5.36 Å as taken from the X-ray structure. This distance measurement is shown schematically in Figure 4. This is the distance which we used to approximate the length of an appropriate spacing group that could take advantage of the accessibility of Phe^{41} and which could act as a hydrogen donor to effectively hydrogen bond with the carbonyl of Phe^{41}. As is seen in Figure 5 the distance from the carbon of the P_1-CO of the inhibitor **17b** to the oxygen of the carbonyl of Phe^{41} is 5.78 Å compared to 5.36 Å for OMTKY3. The spacing group which we employed to elongate **17b** into the P_3' region was Gly-Gly. By incorporating this fragment the inhibitor **23b** was obtained (Figure 6A). The distance from the carbon of the P_1-CO of **23b** to the P_3'-NH of **23b** is 5.44 Å, which is in the range described above to potentially hydrogen bond with the carbonyl of Phe^{41} (see Figure 6A). The P_3'-NH of **23b** acts as a hydrogen donor while the carbonyl of Phe^{41} acts as a hydrogen acceptor. The distance of this hydrogen bond is 1.99 Å. Figure 7 depicts the minimized structure of the complexation of HLE with the inhibitor **23b** (Gly-Gly spacing group) detailing the binding and catalytic sites of HLE. For minimization calculations the

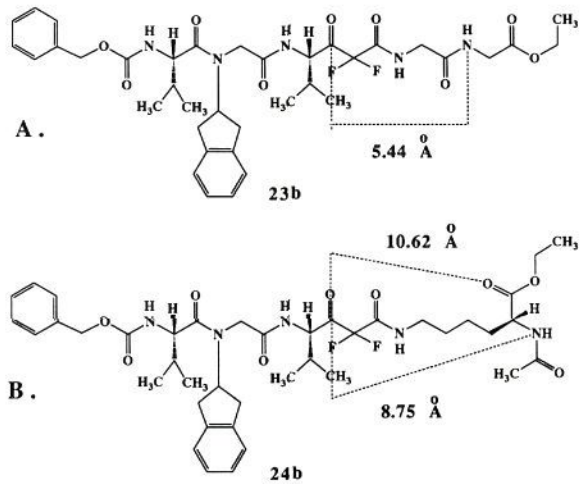

Figure 6. Schematic representations of (a) the distance from the C of the P_1-CO of **23b** to the P_2'-N of **23b**, 5.44 Å, and (b) the distance from the C of the P_1-CO of **24b** to the P_3-O of **24b**, 10.62 Å, and from the C of the P_1-CO of **24b** to the P_3'-N of **24b**, 8.75 Å.

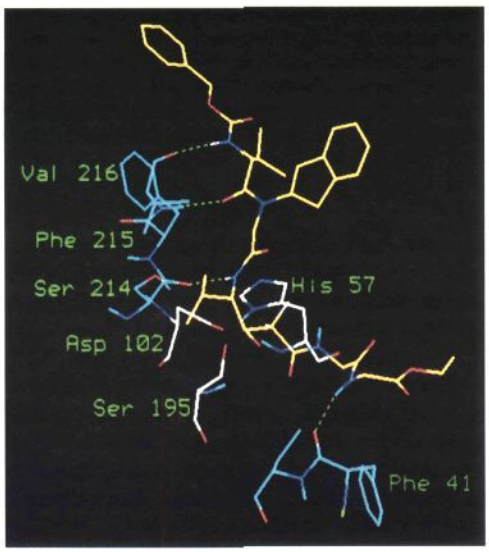

Figure 7. Minimized structure of the complexation of HLE with the inhibitor **23b** (Gly-Gly) in yellow detailing the binding and catalytic sites. The binding residues (Phe^{41}, Ser^{214}, Phe^{215}, and Val^{216}) and the catalytic triad (Ser^{195}, His^{57}, Asp^{102}) are given in blue and white, respectively. For minimization calculations the constraint (1.78 Å) of covalently linking Ser^{195} with the α,α-difluoromethylene carbonyl of the inhibitor **23b**. Hydrogen bonds formed between HLE residues and those of the inhibitor **23b** are indicated by dotted lines (Phe^{41} CO to NH of P_3'-Gly, 1.99 Å; Val^{216} CO to NH of P_3-Val, 1.82 Å; Val^{216} NH to CO of P_3-Val, 1.93 Å; Ser^{214} CO to NH of P_1-Val, 1.84 Å).

constraint (1.78 Å) of covalently linking Ser^{195} with the α,α-difluoromethylene carbonyl of the inhibitor **23b** was made. The hydrogen-bonding distances formed between HLE residues and those of the inhibitor **23b** are as follows: Phe^{41} CO to NH of P_3'-Gly, 1.99 Å; Val^{216} CO to NH of P_3-Val, 1.82 Å; Val^{216} NH to CO of P_3-Val, 1.93 Å; Ser^{214} NH to NH of P_1-Val, 1.84 Å. The corresponding hydrogen-bonding angles between the inhibitor **23b** and HLE are as follows: Phe^{41} CO to N of P_3'-Gly, 139.78°; Phe^{41} O to NH of P_3'-Gly, 151.80°; Val^{216} CO to H of P_3-Val, 165.26°; Val^{216} O to HN of P_3-Val, 171.66°; Val^{216} NH to O of P_3-Val, 166.99°; Val^{216} H to OC of P_3-Val, 163.65°; Ser^{214} CO to H of P_1-Val, 158.06°; Ser^{214} O to HN of P_1-Val, 146.77°. These results correspond to the inhibitor

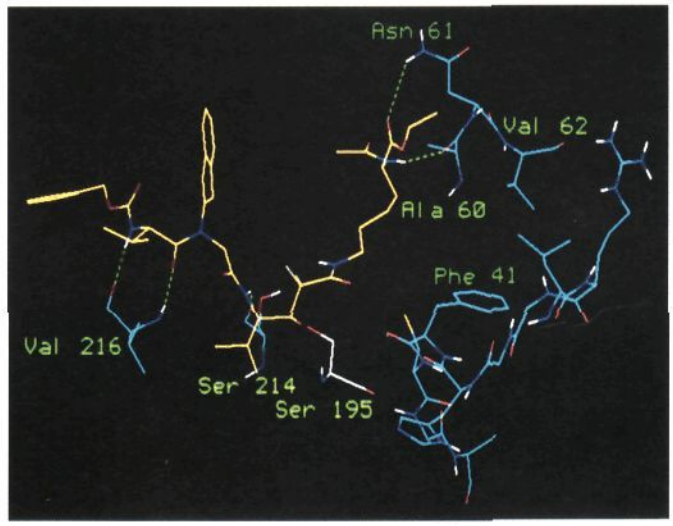

Figure 8. Minimized structure of the complexation of HLE with the inhibitor **24b** in yellow detailing the binding and catalytic sites. The binding residues (Ala^{60}, Asn^{61}, Ser^{214}, Phe^{215}, and Val^{216}) and the catalytic triad (Ser^{195}, His^{57}, and Asp^{102}) are given in blue and white, respectively. For minimization calculations the constraint (1.78 Å) of covalently linking Ser^{195} with the (α,α-difluoromethylene)carbonyl of the inhibitor **24b** via hemiketal formation was utilized. Hydrogen bonds formed between HLE residues and those of the inhibitor **24b** are indicated by dotted lines (Ala^{60} CO to P_3'-NH, 1.89 Å; Asn^{61} NH to CO of P_3'-CO, 3.22 Å; Ser^{214} CO to NH of P_1-Val, 1.88 Å; Val^{216} CO to NH of P_3-Val, 1.84 Å; Val^{216} NH to CO of P_3-Val, 1.87 Å).

23b having one further hydrogen bond than **17b**. This extra hydrogen bond results in a factor of 10 in the relative in vitro potencies of the elongated inhibitor **23b** (IC_{50} = 0.069 μM) versus the shorter **17b** (IC_{50} = 0.635 μM).

The X-ray structure of the OMTKY3–HLE complex was further examined to see if there are any accessible residues other than Phe^{41} within 15 Å of the carbon of the P_1-CO of **17b** that might be taken advantage of through effective hydrogen bonding. This examination indicated that the oxygen of Ala^{60} and the side-chain nitrogen of Asn^{61} fit the above criteria, the distances being 10.79 and 14.15 Å, respectively. These distance measurements are shown schematically in Figure 5. The spacing group which we employed to elongate **17b** into the P_3'-region and thus take advantage of the remote residues Ala^{60} and Asn^{61} was N^{α}-acetyllysine ethyl ester, as is seen in Figure 6B. The distance from the carbon of the P_1-CO of **24b** to the P_3'-NH of **24b** is 8.75 Å. The distance from the P_1-CO of **24b** to the P_3'-ester carbonyl of **24b** is 10.63 Å. Figure 8 depicts the minimized structure of the complexation of the inhibitor **24b** (side-chain of L-lysine being used as the spacing group) detailing the binding and catalytic sites. As in the example above, for minimization purposes the constraint (1.78 Å) of covalently linking Ser^{195} with the α,α-difluoromethylene carbonyl of the inhibitor **24b** was made. The hydrogen-bonding distances formed between HLE residues and those of the inhibitor **24b** are as follows: Ala^{60} CO to P_3'-NH, 1.89 Å; Asn^{61} NH to CO of P_3'-CO, 3.22 Å; Ser^{214} CO to NH of P_1-Val, 1.88 Å; Val^{216} CO to NH of P_3-Val, 1.84 Å; Val^{216} NH to CO of P_3-Val, 1.87 Å. The hydrogen-bonding angles between the inhibitor **24b** and HLE are as follows: Ala^{60} CO to H of P_3'-Lys, 135.55°; Ala^{60} O to HN of P_3'-Lys, 156.74°, Asn^{61} NH to O of P_3'-Lys, 143.83°; Asn^{61} H to OC of P_3'-Lys, 154.29°; Ser^{214} CO to H of P_1-Val, 149.11°; Ser^{214} O to HN of P_1-Val, 153.68°; Val^{216} CO to H of P_3-Val, 165.52°; Val^{216}

Table II. Inhibition of Elastase-Induced Pulmonary Hemorrhage (EPH) in Hamsters by Selected Agents

compd[a]	dose, μg/mL (it.)	N[b]	max % reduction in hemorrhage[c]
17a	NT		
17b	20	4	51.9
19	20	4	55.8
22a	10	4	12.2
22b	20	4	55.2
22c	10	4	94.6
23b	20	4	33.3
24b	20	4	7.6
3[d]	3	4	58.1
	10	4	90.5

[a] Compounds were administered intratracheally (it.) in a 0.1-mL volume (DMSO, 1:100 in saline) followed 5 min later by 50 μg (it.) of HLE in 0.1 mL of saline. [b] Number of animals. [c] Average percent reduction of red blood cells (RBC) per milliliter of cell suspension over vehicle control. [d] Literature[10] ED_{50} = 3.8 μg/animal.

O to HN of P_3-Val, 167.79°. Although **24b** contains one hydrogen bond more than **23b** (IC_{50} = 0.069 μM), there is only a slight enhancement of in vitro potency of **24b** (IC_{50} = 0.057 μM). This is probably due to the fact that the hydrogen bond between the P_3'-CO of **24b** and the side-chain nitrogen of Asn[61] is weak (3.22 Å) and is not of an optimal value.

The results pertaining to the inhibition of elastase-induced pulmonary hemorrhage (EPH) in hamsters by selected representative agents are presented in Table II. HLE induces acute hemorrhage in the hamster[24] lung when administered intratracheally (it.). Hemorrhage can be quantitated 18 h later by measuring red blood cell concentration in bronchial alveolar lavage fluid. In this model, it. administration of one of the most potent in vitro inhibitors, **22c** (IC_{50} = 0.404 μM), 5 min prior to HLE challenge, effectively inhibited hemorrhage in a dose-dependent manner, a dose of 10 μg/mL (it.) resulting in a 94.6% inhibition of hemorrhage. We have previously shown[13] in the case of trifluoromethyl ketone containing inhibitors that tripeptides having a CBZ substituent at the amino terminal end, although they may be potent in vitro, translate into inactive compounds in vivo. For example, the corresponding sulfonamide analog **22c** of the in vivo inactive CBZ derivative **17b** is quite active in vivo, exhibiting 94.6% inhibition against hemorrhage at 10 μg/mL it.

In conclusion, the peptides presented in Table I which contain achiral nonproteinogenic N-substituted glycine residues at P_2 in replacement of L-proline and possess a α,α-difluoromethylene ketone derivative of L-valine at P_1-P_1' are effective in vitro HLE inhibitors with IC_{50} values in the submicromolar range. As previously demonstrated, sterically demanding substituents on the P_2-nitrogen have no detrimental effect on in vitro potency. When substitution is made at P_1 by the α,α-difluoromethylene ketones of L-leucine or L-phenylalanine, activity is lost. The described α,α-difluoromethylene tripeptide inhibitors, i.e. **17b**, interact with the S_3-S_1' binding regions of HLE. Additionally the extended inhibitors **23b** and **24b** were designed through molecular modeling to interact with S_3-S_3' binding subsites of HLE. The described in vitro active inhibitors were also evaluated in hamsters in an elastase-induced pulmonary hemorrhage (EPH) model. In this model, it. administration of **22c**, 5 min prior to HLE challenge (10 μg, it.), effectively inhibited hemorrhage (94.6%) in a dose-dependent manner.

(24) Hassal, C. H.; Johnson, W. H.; Kennedy, A. J.; Roberts, N. A. A New Class of Inhibitors of Human Leukocyte Elastase. *FEBS Lett.* **1985**, *183*, 201–204.

Experimental Section

General. All melting points were determined with a Büchi SMP-20 melting point apparatus and are uncorrected. TLC analyses were performed with E. Merck silica gel 60 F-254 plates of 0.25 mm thickness and were visualized with UV, I_2, or ninhydrin spray reagent. Chemical microanalyses for carbon, hydrogen, and nitrogen were conducted by Midwest Laboratories (Indianapolis, IN) and are within ±0.4% of theoretical values. ^1H NMR were determined with Bruker AM 500 (^1H = 500.13 MHz), Bruker AC 270 (^1H = 270.13 MHz), and Bruker WM 250 (^1H = 250.13 MHz) spectrometers using $(CH_3)_4Si$ as an internal standard. Chemical shifts for ^1H NMR signals are reported in ppm downfield from TMS (δ). Fast atom bombardment (FAB) mass spectra were obtained using a Kratos MS 80RFAQ mass spectrometer (Manchester, U.K.) equipped with a Phrasor Scientific (Duarte, CA) Capillatron Fast Atom Gun. Instrument resolution was 1200 ($m/\Delta m$), the accelerating voltage was 3 kV. A 1:1 mixture of glycerol and thioglycerol was used as the FAB matrix. The FAB gun was operated with Xenon at 8 kV and 35 μA emission current. Chemical ionization (CI) mass spectra were obtained using a Finnigan 4023 GC/MS/DS (San Jose, CA) instrument modified for high-pressure operation. Methane (1.5 Torr) or NH_3 (2.0 Torr) was used as reagent gas. Samples were introduced via direct probe, heated ballistically from 50 to 350 °C. The source temperature was 300 °C, the electron energy was 200 eV, and the emission current was 0.1 mA. The mass range, 50–650 Da, was scanned in 1.95 s.

***N*-(2,3-Dihydro-1*H*-inden-2-yl)glycine Ethyl Ester Hydrochloride (14).**[10] Glycine ethyl ester hydrochloride (34.5 g, 0.247 mol) and 2-indanone (25.1 g, 0.19 mol) were dissolved in absolute EtOH (700 mL) and then $NaCNBH_3$ (25.2 g, 0.41 mol) was added portionwise. The reaction was stirred at room temperature for 16 h. The EtOH was removed under reduced pressure and the residue was treated with H_2O. The product was extracted several times into EtOAc. The organic extract was washed sequentially with saturated aqueous solutions of $NaHCO_3$ and NaCl before being dried ($MgSO_4$) and filtered. After concentration in vacuo the oily residue was taken up in Et_2O (300 mL) and then cooled to 10 °C by means of an ice/water bath. Diethyl ether which had previously been saturated with anhydrous hydrogen chloride was slowly added. The precipitated hydrochloride was filtered and washed with chilled Et_2O to afford the title compound **14** (21 g) as a colorless solid: mp 166–168 °C; ^1H NMR (DMSO-d_6) δ 10.1 (s, 2 H, $^+NH_3$), 7.3–7.1 (m, 4 H), 4.3–4.2 (q, 2 H, CH_3), 4.05 (bs, 3 H, CH_2, CH_3), 3.3–3.2 (dd, 4 H, 2 × CH_2 of indanyl), 1.3–1.2 (t, 3 H, CH_3). Anal. ($C_{13}H_{17}NO_2$·HCl) C, H, N.

Method A. *N*-(Carbobenzyloxy)-L-valyl-*N*-(2,3-dihydro-1*H*-inden-2-yl)glycine Ethyl Ester (15a).[10] To a solution of CBZ-L-valine (5.0 g, 0.02 mol) in CH_2Cl_2 (70 mL) were added DMAP (2.44 g, 0.02 mol), **14** (5.1 g, 0.02 mol), and 1-[3-(dimethylamino)propyl]-3-ethylcarbodiimide hydrochloride (WSCDI) (3.83 g, 0.02 mol). The resulting mixture was stirred at room temperature for 16 h. The CH_2Cl_2 was concentrated under reduced pressure and the residue was treated with EtOAc and 1 N aqueous HCl. The organic layer was separated and washed consecutively with 1 N aqueous HCl, 5% aqueous Na_2CO_3, and saturated aqueous NaCl. The EtOAc was dried ($MgSO_4$), filtered, and concentrated in vacuo to give the crude title compound **15a** as a pale yellow oil. The compound was purified by chromatography over silica gel (CH_2Cl_2) to give the title compound **15a** as a colorless oil: MS (CI/CH_4) m/z (relative intensity) 453 (MH^+, 96), 345 (100), 310 (34), 220 (84), 117 (21), 116 (23); ^1H NMR ($CDCl_3$) δ 7.35 (s, 5 H), 7.15 (s, 4 H), 5.6 (d, 1 H), 5.15–5.0 (m, 3 H), 4.8–4.7 (m, 1 H), 4.2–4.1 (m, 3 H), 3.7–3.6 (d, 1 H), 3.4–2.9 (m, 4 H), 2.15–2.0 (m, 1 H), 1.25 (t, 3 H, CH_3), 1.10–0.9 (dd, 6 H, 2 × CH_3 of Val). Anal. ($C_{26}H_{32}N_2O_5$) C, H, N.

Method B. *N*-(Carbobenzyloxy)-L-valyl-*N*-(2,3-dihydro-1*H*-inden-2-yl)glycine (15b).[10] The corresponding CBZ ethyl ester derivative **15a** (13.8 g, 0.0305 mol) was dissolved in EtOH

(200 mL) and then treated with 1 N aqueous KOH (30 mL) in 5-mL portions. The mixture was stirred at room temperature for 16 h. The EtOH was concentrated under reduced pressure and the residue was treated with H_2O. The aqueous mixture was washed three times with EtOAc, and the layers were separated. The aqueous layer was acidified to pH 3 by the dropwise addition of 1 N aqueous HCl. The product was extracted into EtOAc, and the layers were separated. The organic phase was washed with brine, dried ($MgSO_4$), filtered, and concentrated under reduced pressure to afford the pure title compound **15b** as a colorless semisolid (9.1 g): MS (CI/NH_3) m/z (relative intensity) 425 (MH^+, 53), 317 (98), 258 (15), 192 (34); ^1H NMR ($CDCl_3$) δ 10.4 (bs, 1 H, COOH), 7.35 (m, 5 H), 7.2 (s, 4 H), 6.0 (m, 1 H), 5.15–5.0 (m, 3 H), 4.75 (m, 1 H), 3.7–3.6 (dd, 1 H), 3.35–2.85 (m, 4 H), 2.05 (d, 2 H), 1.1–0.9 (dd, 6 H). Anal. ($C_{24}H_{28}N_2O_5$) C, H, N.

Method C. (*tert*-Butoxycarbonyl)-L-valine Methoxymethylamide (5c).[20] Under argon at 0 °C, *N*-*t*-BOC-L-valine (**4c**) (40.0 g, 0.184 mol) was dissolved in CH_2Cl_2 with stirring. To this solution was added 1,1′-carbonyldiimidazole (CDI) (39.70 g, 0.245 mol). After stirring for 0.5 h, a mixture of *N*,*O*-dimethylhydroxylamine hydrochloride (23.88 g, 0.245 mol) and Et_3N (24.77 g, 0.245 mol) was added at 0 °C. After 1 h of stirring at 0 °C, the reaction mixture was left overnight at room temperature. The reaction mixture was washed with 1 N HCl (2×), saturated aqueous Na_2CO_3 (2×), and brine. The CH_2Cl_2 phase was dried ($MgSO_4$), filtered, and concentrated to give the amide **5c** (47.54 g, 99%): ^1H NMR ($CDCl_3$) δ 5.1 (bs, 1 H, NH), 4.7 (m, 1 H, CHCO), 3.8 (s, 3 H, OCH_3), 3.3 (s, 3 H, NCH_3), 2.0 (m, 1 H, $CH(CH_3)_2$), 1.5 (s, 9 H, *t*-Bu), 1.05 (d, 3 H, CH_3), 0.9 (d, 3 H, CH_3). Anal. ($C_{12}H_{24}N_2O_4$) C, H, N.

Method D. (*tert*-Butoxycarbonyl)-L-valinal (6c).[20] To a solution of the amide **5c** (49.46 g, 0.19 mol) in freshly distilled THF (500 mL) under argon at 0 °C was added $LiAlH_4$ (7.21 g, 0.19 mol) in portions over a 0.5-h period. After stirring 15 min in the cold, an aqueous solution of $KHSO_4$ (25.87 g, 0.19 mol) was slowly added. The reaction mixture was filtered through Celite and the filter cake was washed consecutively with 2 N HCl (2×), saturated aqueous Na_2CO_3 (2×), and brine. After drying ($MgSO_4$), filtering, and concentrating, the aldehyde **6c** (32.3 g, 92%) was obtained as an oil: ^1H NMR ($CDCl_3$) δ 9.6 (s, 1 H, CHO), 5.1 (bs, 1 H, NH), 4.2 (m, 1 H, CHCO), 2.1 (m, 1 H, $CH(CH_3)_2$), 1.45 (s, 9 H, *t*-Bu), 1.05 (d, 3 H, CH_3), 0.95 (d, 3 H, CH_3).

Method E. Ethyl 4(*S*)-[(*tert*-Butoxycarbonyl)amino]-2,2-difluoro-3(*RS*)-hydroxy-5-methylhexanoate (7c).[17,18] Ethyl bromodifluoroacetate (1.5 mL) was added to a refluxing suspension of freshly activated Zn (13.62 g, 0.2 mol) in anhydrous THF (100 mL). After 1 min, a solution of *t*-BOC-L-valinal (**6c**) (16.77 g, 0.083 mol) and ethyl bromodifluoroacetate (40.59 g, 0.2 mol) in THF (75 mL) was added at a rate such that a gentle reflux was maintained. At the end of the addition the reaction mixture was refluxed for another 30 min. The reaction mixture was allowed to cool to room temperature and then $KHSO_4$ (28.3 g, 0.21 mol) in H_2O (150 mL) was added. The reaction mixture was stirred for 30 min and was then filtered through Celite to remove the solid suspension. The filter cake was washed well with Et_2O. To the filtrate was added brine (150 mL). The filtrate was extracted with Et_2O (3×). The combined Et_2O extract was dried ($MgSO_4$), filtered, and concentrated in vacuo to afford crude **7c** (R = $CH(CH_3)_2$) (34.3 g) as an oil. The product was further purified by chromatography over silica gel (2% EtOH in CH_2Cl_2) to give pure **7c** (R = $CH(CH_3)_2$) (20.53 g, 76%) as a mixture of diastereomers which was used directly without further separation: ^1H NMR ($CDCl_3$) δ 5.1 (b, 1 H, NH), 4.3 (m, 3 H, CH_2CH_3, CHOH), 4.1–3.3 (m, 2 H, α-CH, OH), 2.1 (m, 1 H, $CH(CH_3)_2$), 1.5 (s, 9 H, 3 × CH_3), 1.3 (t, 3 H, CH_2CH_3), 1.0 (d, 6 H, 2 × CH_3). Anal. ($C_{14}H_{25}F_2NO_5$) C, H, N.

Method F. 4(*S*)-Amino-2,2-difluoro-3(*RS*)-hydroxy-5-methylhexanoate (8c). The *t*-BOC compound **7c** (R = $CH(CH_3)_2$) (5.0 g, 15.4 mol) was dissolved in a mixture (20 mL) of 30% TFA in CH_2Cl_2. The resulting mixture was stirred at room temperature for 90 min. The TFA and CH_2Cl_2 were concentrated in vacuo (<45 °C). The residue was azeotroped with toluene (5×) at 45 °C by means of a rotary evaporator. After drying overnight in vacuo, the trifluoroacetate salt of **8c** (R = $CH(CH_3)_2$) (5.15 g, 98%) was obtained as a tan oil: ^1H NMR ($CDCl_3$) δ 7.6 (b, 3 H, $^+NH_3$), 4.3 (q, 3 H, CH_2CH_3, CHOH), 3.9–3.3 (m, 2 H, α-CH, OH), 2.2 (m, 1 H, $CH(CH_3)_2$), 1.4 (t, 3 H, CH_2CH_3), 1.1 (d, 6 H, 2 × CH_3). Anal. ($C_9H_{17}F_2NO_3 \cdot CF_3COOH$) C, H, N.

Method G. Ethyl 4(*S*)-[[*N*-(Carbobenzyloxy)-L-valyl-*N*-(2,3-dihydro-1*H*-inden-2-yl)glycyl]amino]-2,2-difluoro-3-(*RS*)-hydroxy-5-methylhexanoate (16; R = $CH(CH_3)_2$). Under argon, HOBT (2.39 g, 17.7 mmol) in dry THF (10 mL) was added to a solution of *N*-CBZ-L-valyl-*N*-(2,3-dihydro-1*H*-inden-2-yl)glycine (**15b**) (7.68 g, 17.7 mmol) in CH_2Cl_2 (20 mL) at 0 °C. To this solution was added WSCDI (3.39 g, 17.7 mmol) in CH_2Cl_2 (10 mL). The reaction mixture was stirred at 0 °C for 30 min and then the trifluoroacetate salt **8c** (R = $CH(CH_3)_2$) (5.0 g, 14.7 mmol) in CH_2Cl_2 (10 mL) was added. The reaction mixture was stirred at 0 °C for 30 min and then for 16 h at room temperature. The reaction mixture was diluted with Et_2O. The Et_2O was washed sequentially with 2 N HCl (2×), saturated aqueous Na_2CO_3 (2×), and brine. The organic phase was dried ($MgSO_4$), filtered, and concentrated to afford crude **16** (R = $CH(CH_3)_2$) (10.36 g) as a viscous oily residue. Flash chromatography over silica gel with increasing solvent polarity (15, 20, 25, and 40% $(CH_3)_2CO$ in petroleum ether) afforded pure **16** (R = $CH(CH_3)_2$) (3.02 g, 41%) as a colorless resinous solid: MS (CI/NH_3) m/z (relative intensity) 632 (MH^+, 100); ^1H NMR δ 7.35 (s, 5 H, aromatics), 7.24 (s, 4 H, indanyl aromatics), 6.95 (d, 1 H, NH), 5.5 (m, 1 H, NH), 5.1 (d, 2 H, $PhCH_2$), 5.0 (m, 1 H, indanyl CH), 4.6 (t, 1 H, α-CH), 4.3 (q, 2 H, CH_2CH_3), 4.2–3.6 (m, 5 H, CH_2 of Gly, α-CH, CHOH), 3.2 (m, 4 H, indanyl CH_2), 2.0 (m, 2 H, 2 × $CH(CH_3)_2$), 1.3 (t, 2 H, CH_2CH_3), 1.0 (m, 12 H, 4 × CH_3). Anal. ($C_{33}H_{43}F_2N_3O_7$) C, H, F, N.

Method H. Ethyl 4(*S*)-[[*N*-(Carbobenzyloxy)-L-valyl-*N*-(2,3-dihydro-1*H*-inden-2-yl)glycyl]amino]-2,2-difluoro-3-oxo-5-methylhexanoate (17; R = $CH(CH_3)_2$). To the alcohol **16** (R = $CH(CH_3)_2$) (500 mg, 0.79 mmol) in CH_2Cl_2 (10 mL) was added Dess–Martin periodinane[21] (1.3 g, 3.05 mmol) followed by TFA (100 μL). The reaction mixture was stirred for 3 h at room temperature and then aqueous $NaHSO_3$ was added. The reaction mixture was stirred for 15 min before the aqueous phase was extracted with EtOAc (2×). The combined EtOAc extract was washed with brine, dried ($MgSO_4$), filtered, and concentrated to afford crude **17** (R = $CH(CH_3)_2$) as a pale yellow oil. Preparative TLC (25% $(CH_3)_2CO$ in petroleum ether) provided the pure product **17** (R = $CH(CH_3)_2$) (320 mg) as a colorless oil: MS (CI/NH_3) m/z (relative intensity) 630 (MH^+, 100); ^1H NMR ($CDCl_3$) δ 7.35 (s, 5 H, aromatics), 7.2 (s, 4 H, aromatics), 7.0 (d, 1 H, NH), 5.58 (d, 1 H, NH), 5.1 (d, 2 H, $PhCH_2$), 5.0 (m, 2 H, α-CH, indanyl CH), 4.7 (t, 1 H, α-CH), 4.35 (q, 2 H, CH_2CH_3), 4.0–3.85 (m, 2 H, CH_2 of Gly), 3.3–3.0 (m, 4 H, 2 × CH_2 of indanyl), 2.38 (m, 1 H, $CH(CH_3)_2$), 2.05 (m, 1 H, $CH(CH_3)_2$), 1.3 (t, 3 H, CH_2CH_3), 1.0–0.8 (m, 12 H, 4 × CH_3). Anal. ($C_{33}H_{41}F_2N_3O_7 \cdot H_2O$) C, H, F, N.

Method I. 4(*S*)-[[*N*-(Carbobenzyloxy)-L-valyl-*N*-(2,3-dihydro-1*H*-inden-2-yl)glycyl]amino]-2,2-difluoro-3(*RS*)-hydroxy-5-methylhexanoic Acid (18: R_1 = $CH(CH_3)_2$). To a solution of the ester **16** (R = $CH(CH_3)_2$) (250 mg, 0.413 mmol) in EtOH (10 mL) was added at 50 °C 1 N KOH (0.41 mL). The resulting mixture was stirred at ambient temperature for 2 h and then diluted with H_2O. The reaction mixture was extracted (3×) with Et_2O/petroleum ether (1:1). The aqueous phase was acidified with 2 N HCl to pH 3 and then extracted with Et_2O (3×). The combined Et_2O extract was washed with brine, dried ($MgSO_4$), filtered, and concentrated to afford the pure acid **18** (R_1 = $CH(CH_3)_2$) (230 mg, 96%) as a colorless resinous solid: ^1H NMR ($CDCl_3$) δ 7.3 (bs, 5 H, aromatics), 7.15 (bs, 4 H, aromatics), 6.0 (m, 1 H, NH), 5.1 (m, 3 H, $PhCH_2$, indanyl CH), 4.8–3.9 (m, 5 H, α-CH of Val, CHOH, CH_2 of Gly), 3.2 (m, 4 H, 2 × CH_2 of indanyl), 2.0 (m, 2 H, 2 × $CH(CH_3)_2$), 0.9 (m, 12 H, 4 × CH_3). Anal. ($C_{31}H_{39}F_2N_3O_7$) C, H, F, N.

4(*S*)-[[*N*-(Carbobenzyloxy)-L-valyl-*N*-(2,3-dihydro-1*H*-inden-2-yl)glycyl]amino]-2,2-difluoro-3-oxo-5-methylhexanoic Acid (19; R_1 = $CH(CH_3)_2$). A procedure similar to method H was followed on a 230-mg (0.38 mmol) scale. After workup, crude **19** (R_2 = $CH(CH_3)_2$) (210 mg) was obtained. Purification by preparative TLC over silica gel (0.5% HOAc and 3% EtOH in CH_2Cl_2) provided pure **19** (90 mg, 40%) as a colorless resinous solid: MS (FAB) (gly/thio) m/z (relative intensity) 640 (MH^+ + K^+, 20), 602 (MH^+, 80); ^1H NMR ($CDCl_3$) δ 7.4 (m, 5 H, aromatics), 7.1 (m, 4 H, aromatics). Anal. ($C_{31}H_{36}F_2N_3O_7K$) C, H, F, N, K.

Method J. Methyl N^6-[4(*S*)-[(*tert*-Butoxycarbonyl)amino]-2,2-difluoro-3(*RS*)-hydroxy-5-methylhexanoyl]-6-amino-2(*S*)-(aminoacetyl)hexanoate (11; R = CH(CH$_3$)$_2$). A mixture of the ester **7c** (R = CH(CH$_3$)$_2$) (500 mg, 1.54 mmol), N^α-acetyl-L-lysine methyl ester (1.83 g, 7.68 mmol), and (*i*-Pr)$_2$NEt (990 mg, 7.65 mmol) in CH$_3$OH (10 mL) was refluxed for 48 h. The reaction was concentrated in vacuo and to the residue was added EtOAc. The EtOAc was washed with brine (3×), dried (MgSO$_4$), filtered, and concentrated to give the pure title amide **11** (R = CH(CH$_3$)$_2$) (660 mg, 89%) as a pale yellow oil: ^{1}H NMR (CDCl$_3$) δ 7.4 (m, 1 H, NH), 7.0 (m, 1 H, NH), 5.2 (m, 2 H, indanyl CH, NH), 4.7–4.2 (m, 3 H, α-CH of lysine, CHCHOH, OH), 2.2 (m, 4 H, α-CH of Val, NHCOCH$_3$), 1.6–1.0 (m, 21 H, *t*-Bu, 3 × CH$_2$, 2 × CH$_3$). Anal. (C$_{21}$H$_{37}$F$_2$N$_3$O$_7$) C, H, N.

Method K. Methyl N^6-[4(*S*)-[[*N*-(Carbobenzyloxy)-L-valyl-*N*-(2,3-dihydro-1*H*-inden-2-yl)glycyl]amino]-2,2-difluoro-3(*RS*)-hydroxy-5-methylhexanoyl]-6-amino-2(*S*)-(aminoacetyl)hexanoate (24a). To the *t*-BOC amine **11** (R = CH(CH$_3$)$_2$) (500 mg, 1.04 mmol) was added at room temperature a mixture (2 mL) of 30% TFA in CH$_2$Cl$_2$. The reaction was stirred at room temperature for 90 min. The reaction was concentrated in vacuo (<45 °C) and azeotroped (3×) with toluene to afford the trifluoroacetate amine salt **12** (R = CH(CH$_3$)$_2$) as a pale yellow oil (590 mg), which was used directly without further purification. The TLC analysis indicated clean transformation to the amine **12**. The coupling of *N*-CBZ-L-valyl-*N*-(2,3-dihydro-1*H*-inden-2-yl)glycine (**15b**) (530 mg, 1.25 mmol) with the trifluoroacetate salt **12** (R = CH(CH$_3$)$_2$) described above was done in a similar manner to that described in method G to give crude **24a** (930 mg) as an oil. Flash chromatography over silica gel (2% CH$_3$OH in CH$_2$Cl$_2$) provided pure **24a** (530 mg, 65%) as a colorless resinous solid: MS (CI/NH$_3$) *m/z* (relative intensity) 788 (MH$^+$, 100); ^{1}H NMR (CDCl$_3$) δ 8.5 (m, 1 H, NH), 8.2 (m, 1 H, NH), 7.5 (m, 1 H, NH), 7.2 (s, 5 H, aromatics), 7.15 (m, 4 H, aromatics), 6.0 (m, 1 H, NH), 5.2–5.0 (m, 3 H, PhCH$_2$, indanyl CH), 4.5–4.1 (m, 4 H, α-CH of Val, α-CH of Lys, CH$_2$ of Gly), 3.8–3.6 (m, 4 H, CHOH, OCH$_3$), 3.3 (m, 6 H, NHCOCH$_3$, indanyl CH$_2$, CHCHOH), 3.0 (m, 4 H, indanyl CH$_2$, CONHCH$_2$), 2.0 (m, 2 H, β-CH of Val), 1.7–1.2 (m, 6 H, 3 × CH$_2$), 0.9 (m, 12 H, 4 × CH$_3$). Anal. (C$_{40}$H$_{55}$F$_2$N$_5$O$_9$·H$_2$O) C, H, N.

Methyl N^6-[4(*S*)-[[*N*-(Carbobenzyloxy)-L-valyl-*N*-(2,3-dihydro-1*H*-inden-2-yl)glycyl]amino]-2,2-difluoro-3-oxo-5-methylhexanoyl]-6-amino-2(*S*)-(aminoacetyl)hexanoate (24b). Following a procedure similar to that described in method H, the alcohol **24a** (400 mg, 0.508 mmol) was oxidized to afford, after workup, the crude ketone **24b** (390 mg). Preparative TLC purification over silica gel (4% CH$_3$OH in CH$_2$Cl$_2$) provided after double development pure **24b** (274 mg, 69%) as a colorless resinous material: MS (CI/NH$_3$) *m/z* (relative intensity) 786 (MH$^+$, 100); ^{1}H NMR (CDCl$_3$) δ 9.1 (m, 1 H, NH), 8.2 (m, 2 H, 2 × NH), 7.5 (m, 1 H, NH), 7.35 (s, 5 H, aromatics), 7.15 (m, 4 H, aromatics), 5.15 (m, 1 H, indanyl CH), 5.03 (d, 2 H, PhCH$_2$), 4.8 (m, 1 H, α-CH of Val), 4.47 (m, 1 H, NHCHOCF$_2$), 4.1 (m, 2 H, CH$_2$ of Gly), 3.75 (m, 1 H, α-CH of Lys), 3.6 (s, 3 H, OCH$_3$), 3.37 (s, 3 H, NHCOCH$_3$), 3.1 (m, 6 H, 2 × CH$_2$ of indanyl, CONHCH$_2$), 2.23 (m, 1 H, β-CH of Val), 2.0 (m, 1 H, β-CH of Val), 1.6–1.27 (m, 6 H, 3 × CH$_2$), 0.9–0.8 (m, 12 H, 4 × CH$_3$). Anal. (C$_{40}$H$_{53}$F$_2$N$_5$O$_9$) C, H, F, N.

Method L. [4(*S*)-[(*tert*-Butoxycarbonyl)amino]-2,2-difluoro-3(*RS*)-hydroxy-5-methylhexanoyl]glycylglycine Ethyl Ester (9; R = CH(CH$_3$)$_2$). A diastereomeric mixture of the alcohol **7c** (R = CH(CH$_3$)$_2$) (500 mg, 1.54 mmol) was dissolved in absolute EtOH (10 mL). To this solution was added glycylglycine ethyl ester (1.51 g, 7.68 mmol) and *i*-Pr$_2$NEt (990 mg, 7.68 mmol). The resulting mixture was refluxed for 48 h. The reaction was concentrated in vacuo and the residue was treated with EtOAc. The EtOAc was washed with brine (3×), dried (MgSO$_4$), filtered, and concentrated to afford the pure amide **9** (R = CH(CH$_3$)$_2$) (570 mg, 84%): ^{1}H NMR (CDCl$_3$) δ 7.85 (m, 2 H, 2 × NH), 5.4 (m, 1 H, NH), 4.4–3.7 (m, 9 H, α-CH of Val, CHOH, 2 × CH$_2$ of Gly, OCH$_2$CH$_3$, OH), 2.0 (m, 1 H, CH(CH$_3$)$_2$), 1.5 (s, 9 H, *t*-Bu), 1.35–1.0 (m, 9 H, CH$_2$CH$_3$, 2 × CH$_3$). Anal. (C$_{18}$H$_{31}$F$_2$N$_3$O$_7$) C, H, N.

[4(*S*)-[[*N*-(Carbobenzyloxy)-L-valyl-*N*-(2,3-dihydro-1*H*-inden-2-yl)glycyl]amino]-2,2-difluoro-3(*RS*)-hydroxy-5-methylhexanoyl]glycylglycine Ethyl Ester (23a). The *t*-BOC amine **9** (R = CH(CH$_3$)$_2$) (550 mg, 1.25 mmol) was added at room temperature to a mixture of 30% TFA in CH$_2$Cl$_2$. The reaction mixture was stirred at room temperature for 2 h. The reaction was concentrated in vacuo (<45 °C) and the residue was azeotroped with toluene (3×) to afford the crude trifluoroacetate salt of the amine **10** (R = CH(CH$_3$)$_2$) (640 mg) as a yellow oil. This material was used directly without further purification. The coupling of the trifluoroacetate salt of **10** (R = CH(CH$_3$)$_2$) (640 mg, 1.5 mmol) with *N*-CBZ-L-valyl-*N*-(2,3-dihydro-1*H*-inden-2-yl)glycine (**15b**) (850 mg, 2.0 mmol) was carried out according to method G to give crude **23a** (1.29 g) as an oil. Purification by flash chromatography over silica gel (1, 2, and 3% EtOH in CH$_2$Cl$_2$) provided pure **23a** (450 mg, 48%) as a colorless resinous solid: MS (CI/C$_4$H$_{10}$) *m/z* (relative intensity) 746 (MH$^+$, 30); ^{1}H NMR (DMSO-*d*$_6$) δ 8.7 (m, 1 H, NH), 8.38 (m, 1 H, NH), 7.5 (m, 1 H, NH), 7.35 (s, 5 H, aromatics), 7.15 (m, 4 H, aromatics), 6.1 (m, 1 H, NH), 5.15–5.0 (m, 3 H, PhCH$_2$, indanyl CH), 4.45 (m, 1 H, α-CH of Val), 4.1 (m, 4 H, OCH$_2$, CHOH, CHCHOH), 3.8–3.65 (m, 6 H, 3 × CH$_2$ of Gly), 3.1–3.0 (m, 4 H, 2 × CH$_2$ of indanyl), 2.0 (m, 1 H, β-CH of Val), 1.8 (m, 1 H, β-CH of Val), 1.2 (t, 3 H, CH$_2$CH$_3$), 0.85 (m, 12 H, 4 × CH$_3$). Anal. (C$_{37}$H$_{49}$F$_2$N$_5$O$_9$·H$_2$O) C, H, F, N.

[4(*S*)-[[*N*-(Carbobenzyloxy)-L-valyl-*N*-(2,3-dihydro-1*H*-inden-2-yl)glycyl]amino]-2,2-difluoro-5-methyl-3-oxohexanoyl]glycylglycine Ethyl Ester (23b). According to method H the alcohol **23a** (300 mg, 0.402 mmol) was converted via Dess–Martin[21] oxidation to the difluoro ketone **23b**. After workup, **23b** (300 mg) was obtained as an oil. Preparative TLC over silica gel (4% EtOH in CH$_2$Cl$_2$) provided pure **23b** (205 mg) as a colorless resin: MS (CI/C$_4$H$_{10}$) *m/z* (relative intensity) 744 (MH$^+$, 100); ^{1}H NMR (DMSO-*d*$_6$) δ 9.3 (m, 1 H, NH), 8.45 (m, 1 H, NH), 8.15 (m, 1 H, NH), 7.5 (m, 1 H, NH), 7.35 (s, 5 H, aromatics), 7.15 (m, 4 H, aromatics), 5.18–5.03 (m, 3 H, PhCH$_2$, indanyl CH), 4.8 (m, 1 H, α-CH of Val), 4.45 (m, 1 H, α-CH of Val), 4.1–3.8 (m, 8 H, CH$_2$CH$_3$, 3 × CH$_2$ of Gly), 3.0 (m, 4 H, 2 × CH$_2$ of indanyl), 2.25 (m, 1 H, β-CH of Val), 1.95 (m, 1 H, β-CH of Val), 1.18 (t, 3 H, CH$_2$CH$_3$), 0.9–0.77 (m, 12 H, 4 × CH$_3$). Anal. (C$_{37}$H$_{47}$F$_2$N$_5$O$_9$·H$_2$O) C, H, F, N.

(*tert*-Butoxycarbonyl)-L-phenylalanine Methoxymethylamide (5a; R = PhCH$_2$).[20] By means similar to that described in method C the methoxymethylamide **5a** was obtained (98%) as a colorless oily material: ^{1}H NMR (CDCl$_3$) δ 7.3 (s, 5 H, Ph), 5.2–4.9 (m, 2 H, α-CH of Phe, NH), 3.7 (s, 3 H, NOCH$_3$), 3.2 (s, 3 H, NCH$_3$), 3.0 (dd, 2 H, β-CH$_2$ of Phe), 1.5 (s, 9 H, *t*-Bu).

(*tert*-Butoxycarbonyl)-L-phenylalanal (6a; R = PhCH$_2$).[20] By means similar to method D the aldehyde **6a** was obtained as a colorless solid (28.44 g, 70%): mp 80–83 °C (lit.[20] mp 86 °C); ^{1}H NMR (CDCl$_3$) δ 9.6 (s, 1 H, CHO), 7.5 (s, 5 H, aromatic), 5.0 (b, 1 H, NH), 4.4 (m, 1 H, α-CH), 3.1 (d, 2 H, PhCH$_2$), 1.4 (s, 9 H, *t*-Bu).

Ethyl 4(*S*)-[(*tert*-Butoxycarbonyl)amino]-2,2-difluoro-3-(*RS*)-hydroxy-5-phenylpentanoate (7a; R = PhCH$_2$). A suspension of freshly activated Zn (13.11 g, 0.2 mol) in freshly distilled dry THF was brought to reflux under argon. To this suspension was added BrCF$_2$CO$_2$Et (1.5 mL). After 1 min a mixture of *t*-BOC-L-phenylalanal (**6a**) (20.0 g, 0.08 mol) and BrCF$_2$CO$_2$Et (39.08 g, 0.19 mol) in THF (75 mL) was added at a rate such that a gentle reflux was maintained. After the addition was complete the reaction mixture was refluxed for an additional 30 min. The reaction mixture was cooled to room temperature and then KHSO$_4$ (27.37 g, 0.2 mol) in H$_2$O (150 mL) was added and the resulting mixture was stirred for 30 min. The reaction mixture was filtered through Celite and the filter cake was washed with EtOAc followed by brine (150 mL). The aqueous phase was extracted with EtOAc (2×). The combined EtOAc extract was dried over MgSO$_4$, filtered, and concentrated to give a brown oil (34.7 g). The oil was filtered through silica gel and eluted with 2% EtOH in CH$_2$Cl$_2$ to afford three fractions. Fractions 1 and 2 provided the desired pure product (**7a**; R = PhCH$_2$) as a colorless oil (13.53 g, 45%): ^{1}H NMR (CDCl$_3$) δ 7.2 (m, 6 H, 5 H, aromatics, NH), 4.88 (d, 1 H, CHOH), 4.3–4.0 (m, 4 H, CH$_2$CH$_3$, α-CH, OH), 3.0 (m, 2 H, PhCH$_2$), 1.4 (s, 9 H, 3 × CH$_3$), 1.3 (t, 3 H, CH$_2$CH$_3$). Anal. (C$_{18}$H$_{25}$F$_2$NO$_5$) C, H, F, N.

Ethyl 4(*S*)-Amino-2,2-difluoro-3(*RS*)-hydroxy-5-phenylpentanoate (8a; R = PhCH$_2$). To a solution (15 mL) of 30% TFA in CH$_2$Cl$_2$ was added **7a** (R = PhCH$_2$) (3.65 g, 9.78 mmol)

and the resulting solution was stirred at 0 °C for 1 h. The reaction was concentrated (<55 °C) in vacuo to afford a syrupy residue (4.83 g) which was identified to be **8a** (R = $PhCH_2$). This material was used directly in the next reaction without further purification: ^1H NMR ($CDCl_3$) δ 9.3 (bs, 3 H, NH_3), 7.2 (bs, 5 H), 4.3–3.9 (m, 4 H, CH_2CH_3, CHOH, α-CH), 3.14 (m, 3 H, $PhCH_2$, OH), 1.3 (t, 3 H, CH_3).

Ethyl 4(*S*)-[[*N*-(Carbobenzyloxy)-L-valyl-*N*-(2,3-dihydro-1*H*-inden-2-yl)glycyl]amino]-2,2-difluoro-3(*RS*)-hydroxy-5-phenylpentanoate (16; R = $PhCH_2$). To a solution of CBZ-L-valyl-*N*-(2,3-dihydro-1*H*-inden-2-yl)glycine (**15b**) (4.98 g, 11.7 mol) in CH_2Cl_2 (25 mL), cooled to −10 °C under argon, was added HOBT (1.5 g, 11.7 mol) in THF (10 mL) followed by the addition of WSCDI (2.25 g, 11.7 mol) in CH_2Cl_2 (5 mL). After stirring for 30 min at −10 °C the trifluoroacetate salt **8a** (R = $PhCH_2$) (4.83 g, 9.78 mmol) in CH_2Cl_2 (10 mL) was added. The reaction mixture was stirred at −10 °C for 15 min before Et_3N (1.63 g, 11.7 mol) was added. The resulting mixture was stirred at 0 °C for 1 h followed by 2 h at room temperature. The reaction was washed consecutively with 10% aqueous HCl (2×), saturated aqueous $NaHCO_3$ (2×), and brine. The organic phase was dried ($MgSO_4$), filtered, and concentrated to give a brown glassy residue (7.3 g). Flash chromatography over silica gel (3% EtOH in CH_2Cl_2) provided the product **16** (R = $PhCH_2$) as a resin. Further purification of the resin (4.35 g) was achieved by flash chromatography over silica gel utilizing a gradient system of 10, 20, and 30% $(CH_3)_2CO$ in petroleum ether. In this manner pure **16** (R = $PhCH_2$) (2.9 g, 44%) was obtained from the 30% $(CH_3)_2CO$/petroleum ether fraction as a colorless amorphous solid: ^1H NMR ($CDCl_3$) δ 7.4–7.1 (m, 14 H, aromatics), 6.1 (b, 1 H, OH), 5.6 (d, 1 H, NH), 5.5 (m, 1 H, indanyl CH), 5.2–5.0 (m, 4 H, $PhCH_2$, CHOH, NH), 4.7 (m, 1 H, α-CH), 4.2–3.8 (m, 4 H, α-CH_2 of Gly, CH_2CH_3), 3.4–2.9 (m, 6 H, indanyl CH_2, $PhCH_2$), 2.6 (m, 1 H, CHCHOH), 2.05 (m, 1 H), 1.1–0.9 (m, 9 H, CH_2CH_3, 2 × CH_3). Anal. ($C_{37}H_{43}F_2N_3O_7$) C, H, N.

Method M. Ethyl 4(*S*)-[[L-Valyl-*N*-(2,3-dihydro-1*H*-inden-2-yl)glycyl]amino]-2,2-difluoro-3(*RS*)-hydroxy-5-phenylpentanoate (20; R_2 = CH_2Ph). To a solution of **16** (R = $PhCH_2$) (2.90 g, 4.27 mmol) in absolute EtOH (40 mL) under argon was added 10% Pd/C (290 mg). The resulting mixture was hydrogenated in a Parr shaker at 45 psi/H_2 for 2 days. The reaction mixture was diluted with CH_2Cl_2 and then filtered through Celite. The filter cake was washed well with CH_2Cl_2/EtOH (1:1). The filtrate was concentrated to afford a pale yellow gummy resin (2.23 g). Flash chromatography over silica gel (2.8% EtOH in CH_2Cl_2) provided the pure desired amino compound **20** (R_2 = $PhCH_2$) (1.19 g, 47%) as a mixture of two diastereomers which was used directly without further separation: MS (FAB) *m/z* (relative intensity) 546.3 (MH^+, 100), ^1H NMR ($CDCl_3$) δ 7.3–7.1 (m, 9 H, aromatic), 6.5 (b, 1 H, NH, or OH), 5.5 (m, 1 H indanyl CH_2), 5.1–4.6 (bm, 3 H, CHOH, NH, α-CH), 4.3 (m, 3 H, CH_2CH_3, NHCHCHOH), 4.1–3.8 (m, 3 H, CH_2 of Gly), 3.3–2.5 (m, 7 H, $PhCH_2$, indanyl CH_2, OH), 1.8 (m, 1 H, $CHCH_3$), 1.4 (t, 3 H, CH_2CH_3), 1.0 (m, 6 H, 2 × CH_3).

Method N. Ethyl 4(*S*)-[[[[4-[[[(4-Chlorophenyl)sulfonyl]amino]carbonyl]phenyl]carbonyl]-L-valyl-*N*-(2,3-dihydro-1*H*-inden-2-yl)glycyl]amino]-2,2-difluoro-3(*RS*)-hydroxy-5-phenylpentanoate (21; R_2 = $PhCH_2$). The acid[10,23] *p*-[*p*-Cl(C_6H_4)SO_2NHCO](C_6H_4)COOH (790 mg, 2.2 mmol) was added to dry THF (10 mL) and the stirring mixture was cooled to 0 °C under argon. To this mixture was added HOBT (300 mg, 2.2 mmol) in THF (10 mL) followed by WSCDI (420 mg, 2.2 mmol) in CH_2Cl_2 (10 mL). After 30 min the amine **20** (R_2 = $PhCH_2$) (1.0 g, 1.83 mmol) in CH_2Cl_2 (10 mL) was added while the temperature was maintained at 0 °C. The reaction mixture was stirred at 0 °C for 30 min followed by 2 h at room temperature. The reaction mixture was diluted with EtOAc. The organic phase was washed consecutively with saturated aqueous Na_2CO_3 (2×), 2 N HCl (2×), and brine (2×). The EtOAc phase was dried ($MgSO_4$), filtered, and concentrated to give a yellow resin (1.49 g, 94%) after flash chromatography over silica gel (0.2–10% EtOH in CH_2Cl_2). For analytical purposes a small sample (300 mg) was further purified by preparative TLC (0.5% HOAc and 3% EtOH in CH_2Cl_2). In this manner an analytically pure sample of **21** (R_2 = $PhCH_2$) (164 mg) was obtained as a colorless resinous solid: MS (CI/NH_3) *m/z* (relative intensity) 867 (MH^+, 11); ^1H NMR (DMSO-d_6) δ 8.7 (m, 1 H, NH), 7.9 (bs, 6 H, aromatics), 7.6 (d, 2 H, aromatics), 7.1 (m, 9 H, aromatics), 6.5 (m, 1 H, NH), 5.3 (m, 1 H, indanyl CH), 4.9–4.5 (m, 2 H, α-CH, NH), 4.4–3.3 (m, 5 H, CH_2 of Gly, CH_2CH_3, CHOH), 3.2–2.7 (m, 7 H, indanyl CH_2, $PhCH_2$, CHOH), 2.2 (m, 1 H, $CH(CH_3)_2$), 1.2–0.8 (m, 9 H, m, CH_2CH_3, 2 × CH_3). Anal. ($C_{43}H_{45}ClF_2N_4O_9S$) C, H, Cl, F, N, S.

Ethyl 4(*S*)-[[[[4-[[[(4-Chlorophenyl)sulfonyl]amino]carbonyl]phenyl]carbonyl]-L-valyl-*N*-(2,3-dihydro-1*H*-inden-2-yl)glycyl]amino]-2,2-difluoro-3-oxo-5-phenylpentanoate (22; R_2 = $PhCH_2$). The title compound was prepared by method H. Preparative TLC purification over silica gel (0.5% HOAc, 3% EtOH in CH_2Cl_2) afforded pure **22** (R_2 = $PhCH_2$) as a colorless resin in 60% yield: MS (CI/NH_3) *m/z* (relative intensity) 865 (MH^+, 98); ^1H NMR (DMSO-d_6) δ 8.8–8.6 (m, 2 H, 2 × NH), 7.9 (bs, 6 H, aromatics), 7.6 (d, 2 H, aromatics), 7.1 (m, 9 H, aromatics), 5.2 (m, 1 H, indanyl CH), 4.9–4.6 (m, 2 H, α-CH, NH), 4.3 (m, 2 H, CH_2CH_3), 4.0–3.3 (m, 2 H, CH_2 of Gly), 3.3–2.7 (m, 5 H, $PhCH_2$, 2 × CH_2 of indanyl, α-CH of Phe), 2.2 (m, 1 H, $CH(CH_3)_2$), 1.2 (t, 3 H, CH_3), 0.9 (m, 6 H, $CH(CH_3)_2$). Anal. ($C_{43}H_{43}ClF_2N_4O_9S·H_2O$) C, H, Cl, F, N, S.

Ethyl 4(*S*)-[[L-Valyl-*N*-(2,3-dihydro-1*H*-inden-2-yl)glycyl]amino]-2,2-difluoro-3(*RS*)-hydroxy-5-methylhexanoate (20; R_2 = $CH(CH_3)_2$). To a solution of **16** (R = $CH(CH_3)_2$) (2.0 g, 3.17 mmol) in absolute EtOH (40 mL) was added 10% Pd/C (400 mg). The resulting mixture was hydrogenated (45 psi) for 16 h by means of a Parr shaker. The reaction mixture was diluted with CH_2Cl_2 (40 mL) and filtered through Celite. The filtrate was concentrated in vacuo to give an oily residue (1.84 g). Flash chromatography over silica gel with first 3% and then 8% EtOH in CH_2Cl_2 provided pure **20** (R_2 = $CH(CH_3)_2$) (1.55 g) as a diastereomeric mixture which was used directly without further separation: ^1H NMR ($CDCl_3$) δ 7.2 (bs, 4 H, aromatic), 6.5 (b, 1 H, NH), 5.6 (m, 1 H, CH of indanyl), 4.3 (m, 4 H, OCH_2CH_3, CHOH, α-CH), 4.2–3.5 (m, 4 H, CH_2 of Gly, CHCHOH, OH), 3.2–2.8 (m, 4 H, 2 × CH_2 of indanyl), 1.8 (m, 2 H, 2 × $CH(CH_3)_2$), 1.3 (t, 3 H, CH_2CH_3), 0.9 (m, 12 H, 4 × CH_3). Anal. ($C_{25}H_{37}F_2N_3O_5$) C, H, N.

Ethyl 4(*S*)-[[[[4-[[[(4-Chlorophenyl)sulfonyl]amino]carbonyl]phenyl]carbonyl]-L-valyl-*N*-(2,3-dihydro-1*H*-inden-2-yl)glycyl]amino]-2,2-difluoro-3(*RS*)-hydroxy-5-methylhexanoate (21; R_2 = $CH(CH_3)_2$). The acid[10,23] *p*-[*p*-Cl(C_6H_4)SO_2NHCO](C_6H_4)COOH (350 mg, 0.965 mmol) was dissolved in dry THF (5 mL) and the resulting solution was chilled to 0 °C and placed under a positive argon atmosphere. To this solution was added HOBT (130 mg, 0.965 mmol) in THF (5 mL) followed by WSCDI (180 mg, 0.965 mmol). After stirring at 0 °C for 30 min the amine **20** (R_2 = $CH(CH_3)_2$) (400 mg, 0.804 mmol) in CH_2Cl_2 (5 mL) was added. The resulting mixture was stirred at 0 °C for 45 min followed by 1 h at room temperature. The reaction mixture was diluted with Et_2O and then washed sequentially with saturated aqueous $NaHCO_3$ (2×), 2 N HCl (2×), and brine. The organic phase was dried ($MgSO_4$), filtered, and concentrated to give crude **21** (R_2 = $CH(CH_3)_2$) (710 mg) as a white colorless resin. Preparative TLC over silica gel (0.5% HOAc and 5% EtOH in CH_2Cl_2) provided pure **21** (R_2 = $CH(CH_3)_2$) (520 mg) as a colorless white powder: MS FAB (gly/thio) *m/z* (relative intensity) 819 (MH^+, 80); ^1H NMR ($CDCl_3$) δ 10.5 (bs, 1 H, SO_2NH), 8.1 (m, 2 H, aromatics), 7.8 (m, 4 H, aromatics), 7.5 (m, 2 H, aromatics), 7.3 (m, 1 H, NH), 7.2 (m, 4 H, aromatics), 6.8 (d, 1 H, NH), 5.2 (m, 1 H, CH of indanyl), 5.1 (m, 1 H, α-CH), 4.3–3.8 (m, 5 H, OCH_2CH_3, CH_2 of Gly, CHOH), 3.4–3.1 (m, 5 H, 2 × CH_2 of indanyl, CHCHOH), 2.3–1.8 (m, 3 H, 2 × $CH(CH_3)_2$, OH), 1.3 (t, 3 H, CH_2CH_3), 1.1–0.7 (m, 12 H, 4 × CH_3). Anal. ($C_{39}H_{45}ClF_2N_4O_9S$) C, H, Cl, F, N, S.

Method O. Ethyl 4(*S*)-[[[[4-[[[(4-Chlorophenyl)sulfonyl]amino]carbonyl]phenyl]carbonyl]-L-valyl-*N*-(2,3-dihydro-1*H*-inden-2-yl)glycyl]amino]-2,2-difluoro-3-oxo-5-methylhexanoate (22; R_2 = $CH(CH_3)_2$). To the alcohol **21** (R_2 = $CH(CH_3)_2$) (1.14 g, 1.39 mmol) in CH_2Cl_2 (25 mL) was added Dess–Martin periodinane[21] (2.18 g, 5.15 mmol) followed by TFA (110 μL). The reaction mixture was stirred at room temperature for 3 h before a saturated aqueous mixture of $Na_2S_2O_3$ and $NaHCO_3$ was added. The resulting mixture was stirred for 30 min. The aqueous mixture was extracted several times with EtOAc (3×). The combined EtOAc extract was washed with 10% aqueous HCl and then with brine. The EtOAc was dried

($MgSO_4$), filtered, and concentrated to afford crude **22** (R_2 = $CH(CH_3)_2$) (1.2 g) as a yellow resin. Flash chromatography over silica gel (0.5% HOAc and 2% EtOH in CH_2Cl_2) gave pure **22** (R_2 = $CH(CH_3)_2$) (520 mg) as a colorless resin: MS FAB (gly/thio) *m/z* (relative intensity) 817 (MH^+, 80); ^1H NMR (DMSO-d_6) δ 8.75 (d, 1 H, SO_2NH), 8.6 (m, 1 H, NH), 8.2 (d, 1 H, NH), 7.9 (m, 6 H, aromatics), 7.6 (d, 2 H, aromatics), 7.15 (m, 4 H, aromatics), 5.3 (m, 1 H, indanyl CH), 4.9 (m, 1 H, α-CH), 4.65 (m, 1 H, α-CH), 4.3 (q, 2 H, OCH_2CH_3), 3.6 and 4.1 (2 dd, 2 H, CH_2 of Gly), 3.2–3.0 (m, 4 H, 2 × CH_2 of indanyl), 2.2 (m, 2 H, 2 × $CH(CH_3)_2$), 1.2 (t, 3 H, CH_2CH_3), 1.0–0.8 (m, 12 H, 4 × CH_3). Anal. ($C_{39}H_{43}ClF_2N_4O_9S$) C, H, Cl, F, N, S.

(*tert*-Butoxycarbonyl)-L-leucine Methoxymethylamide (5b; R = $CH_2CH(CH_3)_2$).[20] By a procedure similar to method C the methoxymethylamide **5b** was obtained in 86% yield as a colorless oil: ^1H NMR ($CDCl_3$) δ 5.2–4.6 (m, 2 H, CHCO, NH), 4.74 (s, 3 H, $N(OCH_3)$), 3.24 (s, 3 H, NCH_3), 1.6–1.4 (m, 3 H, CH_2 $CH(CH_3)_2$), 1.5 (s, 9 H, *t*-Bu), 1.05 (d, 3 H, CH_3), 0.9 (d, 3 H, CH_3).

(*tert*-Butoxycarbonyl)-L-leucinal (6b; R = $CH_2CH(CH_3)_2$).[20] By a procedure similar to method D the aldehyde **6b** was obtained in 75% yield as a colorless viscous oil: ^1H NMR ($CDCl_3$) δ 9.64 (s, 1 H, CHO), 5.0 (m, 1 H, NH), 4.25 (m, 1 H, CH), 2.0–1.35 (m, 3 H, CH_2, $CH(CH_3)_2$), 1.45 (s, 9 H, *t*-Bu), 1.0 (d, 6 H, 2 × CH_3).

Ethyl 4(*S*)-[(*tert*-Butyloxycarbonyl)amino]-2,2-difluoro-3(*RS*)-hydroxy-6-methylheptanoate (7b; R = $CH_2CH(CH_3)_2$). A stirred suspension of freshly activated Zn (17.08 g, 0.26 mol) in dry THF (150 mL) was placed under nitrogen and then bromodifluoroacetate (1.5 g) was added. The mixture was heated to a gentle reflux. After 1 min a mixture of *t*-BOC-L-leucinal (**6b**) (22.5 g, 0.1 mol) and ethyl bromodifluoroacetate (49.41 g, 0.25 mol) in THF (100 mL) was added dropwise while a gentle reflux was maintained. At the end of the addition the reaction was further refluxed for 30 min and then cooled to room temperature. To the reaction mixture was added 1 M aqueous $KHSO_4$ (150 mL). The resulting mixture was stirred for 15 min and then filtered through Celite. The filter cake was washed with EtOAc. The organic filtrate was separated and the aqueous phase was extracted with EtOAc (3×). The combined organic extract was washed with brine (150 mL), dried ($MgSO_4$), filtered, and concentrated to give crude **7b** (R = $CH_2CH(CH_3)_2$) (48.14 g). Flash chromatography over silica gel (2% EtOH in CH_2Cl_2) provided pure **7b** (R = $CH_2CH(CH_3)_2$) (21.16 g) as an oil: ^1H NMR ($CDCl_3$) δ 4.7 (bs, 1 H, NH), 4.4 (m, 1 H, CHOH), 4.35 (q, 2 H, OCH_2CH_3), 4.1–3.85 (m, 2 H, CHCHOH, OH), 1.7 (m, 3 H, β-CH, $CH(CH_3)_2$), 1.4 (m, 9 H, *t*-Bu), 1.35 (t, 3 H, CH_2CH_3), 0.9 (m, 6 H, 2 × CH_3). Anal. ($C_{15}H_{27}F_2NO_5$) C, H, N.

Ethyl 4(*S*)-Amino-2,2-difluoro-3(*RS*)-hydroxy-6-methylheptanoate Trifluoroacetate Salt (8b; R = $CH_2CH(CH_3)_2$). The *t*-BOC amine **7b** (R = $CH_2CH(CH_3)_2$) (5.0 g, 14.7 mmol) was added to a mixture (20 mL) of 30% TFA in CH_2Cl_2 and the resulting solution was stirred at room temperature for 1 h. The reaction was concentrated in vacuo (<45 °C) and then azeotroped (3×) with toluene to afford a tan oil. The residue was dried for 16 h under vacuum to afford the trifluoroacetate salt **8b** (R = $CH_2CH(CH_3)_2$) (5.88 g) which was used directly without further purification.

Ethyl 4(*S*)-[[*N*-(Carbobenzyloxy)-L-valyl-*N*-(2,3-dihydro-1*H*-inden-2-yl)glycyl]amino]-2,2-difluoro-3(*RS*)-hydroxy-6-methylheptanoate (16; R = $CH_2CH(CH_3)_2$). By means similar to method G, the trifluoroacetate salt **8b** (R = $CH_2CH(CH_3)_2$) (4.89 g, 13.1 mmol) was condensed with *N*-CBZ-L-valyl-*N*-(2,3-dihydro-1*H*-inden-2-yl)glycine (**15b**) (5.6 g, 13.1 mmol). Purification of the crude product was accomplished by flash chromatography over silica gel using a gradient system of 10, 15, 20, and 40% $(CH_3)_2CO$ in petroleum ether. Most of the desired product **16** (R = $CH_2CH(CH_3)_2$) was collected in the 20% $(CH_3)_2CO$ fraction. Fraction 2 afforded a pure diastereomer (3.0 g) as a colorless oil. Fraction 3 was a mixture of diastereomers. The physical data for fraction 2 is as follows: MS FAB (gly/thio) *m/z* (relative intensity) 646 (MH^+, 30); ^1H NMR ($CDCl_3$) δ 7.4 (s, 5 H, aromatics), 7.27 (m, 4 H, aromatics), 5.6 (m, 1 H, NH), 5.2 (m, 3 H, $PhCH_2$, indanyl CH), 4.9 (m, 1 H, α-CH), 4.7–3.9 (m, 6 H, CHOH, OCH_2CH_3, CH_2 of Gly, CHCHOH), 3.3–3.0 (m, 4 H, CH_2 of indanyl), 2.1 (m, 1 H, β-CH of Val), 1.7 (m, 3 H, β-CH_2 of Leu, δ-CH of Leu), 1.4 (t, 3 H, CH_2CH_3), 1.0 (m, 12 H, 4 × CH_3). Anal. ($C_{34}H_{45}F_2N_3O_7$) C, H, F, N.

Ethyl 4(*S*)-[[L-Valyl-*N*-(2,3-dihydro-1*H*-inden-2-yl)-glycyl]amino]-2,2-difluoro-3(*RS*)-hydroxy-6-methylheptanoate (20; R_2 = $CH_2CH(CH_3)_2$). To a solution of the *N*-CBZ peptide **16** (R = $CH_2CH(CH_3)_2$) (2.33 g, 3.61 mmol) in absolute EtOH (40 mL) was added 10% Pd/C (250 mg). The resulting mixture was hydrogenated (45 psi) by means of a Parr apparatus for 16 h. The reaction was filtered through Celite and the filtrate was concentrated in vacuo to give crude amine **20** (R_2 = CH_2-$CH(CH_3)_2$) (1.89 g) as an oil. Purification of the crude product by flash chromatography over silica gel eluting first with 20% $(CH_3)_2CO$ in petroleum ether followed by 3% EtOH in CH_2Cl_2 gave the pure title compound **20** (R_2 = $CH_2CH(CH_3)_2$) (970 mg) as a colorless oil: MS FAB (gly/thio) *m/z* (relative intensity) 512 (MH^+, 50); ^1H NMR ($CDCl_3$) δ 7.2 (m, 4 H, aromatics), 6.1 (m, 1 H, NH), 5.65 (m, 1 H, indanyl CH), 4.6 (m, 1 H, α-CH), 4.35 (m, 2 H, CH_2CH_3), 4.2 (d, 1 H, CHOH), 3.9–3.7 (m, 3 H, CH_2 of Gly, CHCHOH), 3.3–2.8 (m, 5 H, 2 × CH_2 of indanyl, OH), 1.9 (m, 1 H, β-CH of Val), 1.6 (m, 2 H, β-CH of Leu), 1.4 (t, 3 H, CH_2CH_3), 1.3 (m, 1 H, δ-CH of Leu), 1.1–0.90 (m, 12 H, 4 × CH_3). Anal. ($C_{26}H_{39}F_2N_3O_5$) C, H, N.

Ethyl 4(*S*)-[[[[4-[[[(4-Chlorophenyl)sulfonyl]amino]carbonyl]phenyl]carbonyl]-L-valyl-*N*-(2,3-dihydro-1*H*-inden-2-yl)glycyl]amino]-2,2-difluoro-3(*RS*)-hydroxy-6-methylheptanoate (21; R_2 = $CH_2CH(CH_3)_2$). To a chilled (0 °C) solution of the acid[10,23] *p*-[*p*-Cl(C_6H_4)SO_2NHCO](C_6H_4)COOH (800 mg, 2.23 mmol) in THF (10 mL) was added HOBT (300 mg, 2.23 mmol) in THF (100 mL). To this solution was added WSCDI (430 mg, 2.23 mmol) in CH_2Cl_2 (10 mL). The resulting mixture was stirred at 0 °C for 30 min and then a solution of the amine **20** (R_2 = $CH_2CH(CH_3)_2$) (950 mg, 1.86 mmol) in CH_2Cl_2 (10 mL) was added. The resulting mixture was stirred at 0 °C for 30 min and then at room temperature for 2 h. The reaction mixture was diluted with Et_2O and washed sequentially with 2 N HCl (2×), saturated aqueous Na_2CO_3 (2×), and brine. The Et_2O phase was dried ($MgSO_4$), filtered, and concentrated to give crude **21** (R_2 = $CH_2CH(CH_3)_2$) (1.73) as a colorless amorphous solid. Flash chromatography over silica gel (3% EtOH in CH_2Cl_2) provided pure **21** (R_2 = $CH_2CH(CH_3)_2$) (1.41 g, 91%) as a colorless amorphous solid: MS FAB (gly/thio) *m/z* (relative intensity) 855 (MH^+, 40); ^1H NMR (DMSO-d_6) δ 8.7 (m, 1 H, NH), 7.95 (m, 6 H, aromatics), 7.75 (m, 1 H, NH), 7.6 (m, 2 H, aromatics), 7.15 (m, 4 H, aromatics), 6.17 (m, 1 H, NH), 5.3 (m, 1 H, indanyl CH), 4.88 (m, 1 H, α-CH of Val), 4.27 (m, 3 H, OCH_2CH_3, CHOH), 4.0 (m, 2 H, CH_2 of Gly), 3.6–2.9 (m, 6 H, 2 × CH_2 of indanyl, CHCHOH, OH), 2.1 (m, 1 H, β-CH of Val), 1.5 (m, 1 H, δ-CH of Leu), 1.25 (m, 5 H, CH_2CH_3, β-CH_2 of Leu), 1.0–0.8 (m, 12 H, 4 × CH_3). Anal. ($C_{40}H_{46}ClF_2N_4O_9S$·Na) C, H, Cl, F, N, Na.

Ethyl 4(*S*)-[[[[4-[[[(4-Chlorophenyl)sulfonyl]amino]carbonyl]phenyl]carbonyl]-L-valyl-*N*-(2,3-dihydro-1*H*-inden-2-yl)glycyl]amino]-2,2-difluoro-3-oxo-6-methylheptanoate (22; R_2 = $CH_2CH(CH_3)_2$). According to method O the alcohol **21** (R_2 = $CH_2CH(CH_3)_2$) (1.21 g, 1.45 mmol) was converted, via a Dess–Martin periodinane oxidation,[21] to the ketone **22** (R_2 = $CH_2CH(CH_3)_2$). The crude product **22** (1.16 g) was further purified by flash chromatography over silica gel (5% EtOH in CH_2Cl_2) to afford the pure title compound **22** (700 mg, 58%) as a colorless resin: MS FAB (gly/thio) *m/z* (relative intensity) 869 (M + K^+, 100), 831 (MH^+, 80); ^1H NMR ($CDCl_3$ + CF_3COOD) δ 8.1 (d, 2 H, aromatics), 7.9 (s, 4 H, aromatics), 7.6 (d, 2 H, aromatics), 7.2 (m, 6 H, aromatics, NH), 5.3–5.1 (m, 2 H, CH_2 of indanyl, α-CH), 4.4 (q, 3 H, OCH_2CH_3, α-CH of Leu), 4.2–4.0 (dd, 2 H, CH_2 of Gly), 3.5 (m, 2 H, CH_2 of indanyl), 3.1 (m, 2 H, CH_2 of indanyl), 2.2 (m, 1 H, β-CH of Val), 1.8 (m, 1 H, δ-CH of Leu), 1.45 (m, 2 H, β-CH_2 of Leu), 1.35 (t, 3 H, CH_2CH_3), 1.15–0.75 (m, 12 H, 4 × CH_3). Anal. ($C_{40}H_{44}ClF_2N_4O_9S$·K) C, H, Cl, F, N, S.

Ethyl 4(*S*)-[[(*N*-Carbobenzyloxy)-L-valyl-*N*-(2,3-dihydro-1*H*-inden-2-yl)glycyl]amino]-2,2-difluoro-3-oxo-6-methylhexanoate (17; R = $CH_2CH(CH_3)_2$). By means similar to that described in method H the alcohol **16** (R = $CH_2CH(CH_3)_2$) (800 mg, 1.24 mmol) was oxidized to the corresponding ketone **17**. The crude ketone **17** (810 mg) was obtained as an oil. The crude product was purified by flash chromatography over silica gel employing first the solvent system CH_2Cl_2/petroleum ether (1:1) followed by the system 2% EtOH in CH_2Cl_2 to give the pure title compound **17** (R = $CH_2CH(CH_3)_2$) (300 mg, 38%) as a colorless

oil: MS FAB (gly/thio) m/z (relative intensity) 644 (MH^+, 30); ^1H NMR ($CDCl_3$) δ 7.30 (s, 5 H, aromatics), 7.17 (s, 4 H, aromatics), 6.87 (d, 1 H, NH), 5.5 (d, 1 H, NH), 5.3–5.0 (m, 5 H, $PhCH_2$, OCH_2CH_3, α-CH of Val), 4.65 (m, 1 H, α-CH of Leu), 4.3 (m, 3 H, OCH_2CH_3, indanyl CH), 3.9 (m, 2 H, CH_2 of Gly), 3.3–3.0 (m, 4 H, 2 × CH_2 of indanyl), 2.05 (m, 1 H, β-CH of Val), 1.7 (m, 2 H, β-CH_2 of Leu), 1.4 (m, 1 H, δ-CH of Leu), 1.3 (t, 3 H, CH_2CH_3), 0.9 (m, 12 H, 4 × CH_3). Anal. ($C_{34}H_{43}F_2N_3O_7$) C, H, F, N.

Human Leukocyte Elastase (HLE) Inhibition Screen in Vitro. The method of Nakajima was adapted to a microtiter format.[25] The in vitro assay was based upon the hydrolysis of the commercially available (Sigma Chemical Co., St. Louis, MO) substrate MeO-Suc-Ala-Ala-Pro-Val p-nitroanilide and the resulting release of p-nitroanilide (pNA) which absorbs at 405 nm. The release of pNA was followed spectrophotometrically. The equipment used in the assay were microtiter flat bottom plates having 96 wells/plate, a V_{max} kinetic microtiter plate reader equipped with a 405-nm filter (Molecular Devices), a microtiter plate mixer (Fisher Scientific), and a Cary 118 spectrophotometer. Human sputum elastase (HSE) (Elastin Products Co., Owensville, MO) was dissolved at 1 mg/mL in 0.05 M NaCl and frozen (50-μL aliquots) at −20 °C until used. A stock solution of MeO-Suc-Ala-Ala-Pro-Val p-nitroanilide was prepared by dissolving at 15 mM in DMSO and frozen (4-mL aliquots) at −20 °C until used. The assay buffer was 0.1 M Tris buffer, pH 7.5, containing 0.5 M NaCl. Screening was performed in microtiter plates using 0.5 mM of substrate. Enzyme activity (+/− test compound) was determined as the rate of pNA release (linear regression analysis of the slope). The inhibitory activity of the test compound was calculated relative to the uninhibited enzyme control as follows:

$$\% \text{ inhibition} = 100 - \frac{\text{rate (with test compound)} \times 100}{\text{rate (enzyme control)}}$$

A frozen aliquot of HSE was thawed and diluted with the assay buffer to a stock concentration of 0.02 mg/mL (30× the assay concentration). A frozen aliquot of the substrate stock solution was thawed and diluted to 0.5 mM with the assay buffer (the final concentration of DMSO was 10%). A 10-μL sample of the test compound stock solution (or the assay buffer) and 10 μL of the HSE stock solution were pipetted into each microtiter well in duplicate. The plates were well mixed and preincubated at room temperature for 15 min. A substrate solution (300 μL) was then added to each well and the OD_{405} was followed for approximately 30 min.

Elastase-Induced Pulmonary Hemorrhage (EPH) Model in Hamsters. Experiments were conducted using four male, Syrian golden hamsters per group weighing 90–130 g, obtained from Charles River Laboratories. The animals were quarantined for a minimum of 3 days before use during which time they were maintained under routine animal care procedures. Anesthesia required for the intratracheal administration of elastase was induced by ip injection of Nembutal (sodium pentobarbital, 50–100 mg/kg of body weight). Hamsters were anesthetized as described above and the trachea was surgically exposed. Test compounds were solubilized in DMSO at 20 mg/mL and diluted 1:100 in normal saline for a working concentration of 200 μg/mL. The compound or vehicle (DMSO, 1:100 in saline) were administered intratracheally (it.) via a 27-gauge needle, inserted directly into the trachea in 0.1 mL volume (20 μg of compound). Five minutes later, purified human sputum elastase (Elastin Products Co., Owensville, MO), 50 μg in 0.1 mL saline, was administered directly into the trachea. Eighteen hours later animals were sacrificed by an overdose of Nembutal. Whole lung lavage fluid was performed using normal saline at room temperature. A 6-mL sample of lavage fluid was collected from each animal and each sample was assayed for red blood cell (RBC) concentration (manual counts) as a measure of pulmonary hemorrhage. Each 6-mL lavage sample was centrifuged at approximately 1400 rpm for 10 min. The supernatant was discarded and the cell pellet was gently resuspended in 1 mL of normal saline. A 25-μL aliquot of the cell suspension was added to 475 μL of Trypan Blue (1:20 dilution) and manual RBC counts were performed. The number of RBCs/mL of cell suspension was calculated. The percent inhibition of pulmonary hemorrhage was calculated as follows:

$$\% \text{ inhibition} = 100 \times [\text{no. RBC}/(\text{mL vehicle control})] - [\text{no. RBC}/(\text{mL compound tested})]/[\text{no. RBC}/(\text{mL vehicle control})]$$

Statistical analysis[26] of the data was performed using analysis of variance (ANOVA) and Dunnett's multiple comparison test.

Conformational Analysis and Molecular Modeling. Initial optimized geometries of inhibitors were accomplished using the force field program MM2/MMP2 (Molecular Design Ltd. Hayward, CA) of Allinger[27] employing a VAX 11/750 (Boston, MA) computer. In order to model the enzyme–inhibitor interactions, we made use of two experimental X-ray structures corresponding to a complex between HLE and the third domain of the turkey ovomucoid inhibitor (OMTKY3) as well as that of HLE with the inhibitor MeO-Suc-Ala-Ala-Pro-Val-chloromethyl ketone (MPCMK). The X-ray coordinates of both complexes were kindly provided to us by Dr. W. Bode (Max Planck Institute, Martinsried, Germany). The backbone atoms of the previously minimized (MM2/MMP2) structures of the inhibitors were superimposed onto the corresponding atoms of the inhibitors in either X-ray structure. Presumably, the mechanism of inhibition of the enzyme by such inhibitors containing trifluoromethyl ketone moieties lies in the formation of a stable hemiketal between Ser^{195} and the ketone carbonyl of the inhibitor. To simulate this situation in the modeling process, the O^{γ} atom of Ser^{195} and the C atom of the ketone group of the inhibitor were constrained (1.78 Å) to their corresponding positions as observed in the X-ray structure (MPCMK) through the use of a forcing potential. Energy refinement was performed on the "active-site region", which was defined as the region consisting of all residues with any atom within a 15-Å sphere centered on the N atom of the N-substituted glycine residue. In order to avoid large atomic movements resulting in unrealistic distortion or deviation from the initial structure, the energy refinement process was performed in two stages. First, a harmonic forcing potential was applied to every atom in the energy minimization procedure so as to relax bad steric contact and to constrain the structure close to its initial conformation. Second, the forcing potential was slowly relaxed in stages to bring the system to a stable conformation, with a convergence criterion of the maximum derivative being set at 0.01. Typically, a total of about 4000–5000 iteration steps are required for such convergence to occur. Minimizations of the HLE–inhibitor complexes was done using the program CHARMm (Polygen Corp., Waltham, MA) and utilizing a Silicon Graphics 4D/50 (Mountain View, CA) computer. Molecular graphics interpretation of the results was done via QUANTA (Polygen Corp.).

Acknowledgment. We are indebted to S. Campbell, S. Leonard, and T. Saboe for providing ^1H NMR of all new compounds, G. Hanson and K. McKellop for providing mass spectral data, and Professor W. Bode of the Max Planck Institute (Martinsried, Germany) for providing the X-ray coordinates of the complexes of HLE with MPCMK and with OMTKY3.

(25) Nakajima, K.; Powers, J. C.; Ashe, B. M.; Zimmerman, M. Mapping the Extended Substrate Binding Site of Cathepsin G and Human Leukocyte Elastase. *J. Biol. Chem.* **1979**, *254*, 4027–4032.

(26) (a) Blaker, W. D. Computer Program for the Parametric and Nonparametric Comparison of Several Groups to a Control. *Comput. Biol. Med.* **1987**, *17*, 37–44. (b) Kramer, C. Y. Extension of Multiple Range Tests to Group Means with Unequal Numbers of Replications. *Biometrics* **1956**, *12*, 307. (c) SAS Institute Inc., *SAS User's Guide, Version 5 Edition*; SAS Institute Inc.; Cary, NC, 1985; pp 434–506.

(27) (a) Burkert, U.; Allinger, N. L. *Molecular Mechanics*; ACS monograph; American Chemical Society: Washington, DC, 1982. (b) Allinger, N. L. Conformational Analysis 130. MM2. A Hydrocarbon Force Field Utilizing V_1 and V_2 Torsional Terms. *J. Am. Chem. Soc.* **1977**, *99*, 8127–8134.